

Smart Grid Sensor

Akash K Singh, PhD

IBM Corporation Sacramento, USA

Abstract

For century, there has been no change in the fundamental structure of the electrical power grid and vehicle networks. Current hierarchical. centrally controlled grid of the electrical grid is not best for growing demand. To address the challenges of the existing power grid, the new concept of smart grid and smarter planet are under research. The smart grid can be considered as a modern electric power grid infrastructure for enhanced efficiency and reliability through automated control, high-power converters, modern communications infrastructure, sensing and metering technologies, and modern energy management techniques based on the optimization of ondemand, energy and network availability. While current power systems are based on a solid information and communication infrastructure, the new smart grid needs a different and much more complex one, as its dimension is much larger and needs utmost performance. This paper addresses critical issues on smart grid technologies primarily in terms of information and communication technology (ICT) issues and opportunities. The main objective of this paper is to provide a contemporary look at the current state of the art in smart grid communications as well as to discuss the still-open research issues in this field. It is expected that this paper will provide a better understanding of the technologies, potential advantages and research challenges of the smart grid and provoke interest among the research community to further explore this promising research area.

Keywords- Advanced metering infrastructure (AMI), communication technologies, quality-ofservice (QoS), smart grid, standards

I. INTRODUCTION

Electric power grid contains three main subsystems, i.e., power generation, power transmission & distribution, and customer facilities. Recently, wireless sensor networks (WSNs) have been considered as a promising technology that can enhance all these three subsystems, making WSNs an important component of the smart grid. However, environmental noise and interference from nonlinear electric power equipments and fading in harsh smart grid environments, makes reliable communication a challenging task for single-channel WSNs for smart grid applications. To improve network capacity in smart grid environments, multi-channel WSNs might be the preferred solution while achieving simultaneous transmissions through multiple channels. In this paper, the performance of multichannel WSNs is investigated for different spectrum environments of smart power grid, e.g., 500kV outdoor substation, main power control room and underground network transformer vaults. In addition, we also introduce potential applications of multi-channel WSNs along with the related technical challenges. Here, our goal is to envision potential advantages and applications of multichannel WSNs for smart grid and motivate the research community to further explore this promising research area. Sensor network web services have recently emerged as promising tools to provide remote management, data collection and querying capabilities for sensor networks. They can be utilized in a large number of fields among which Demand- Side Energy Management (DSEM) is an important application area that has become possible with the smart electrical power grid. DSEM applications generally aim to reduce the cost and the amount of power consumption. In the traditional power grid, DSEM has not been implemented widely due to the large number of households and lack of fine-grained automation tools. However by employing intelligent devices and implementing communication infrastructure among these devices, the smart grid will renovate the existing power grid and it will enable a wide variety of DSEM applications. In this paper, we analyze various DSEM scenarios that become available with sensor network web services. We assume a smart home with a Wireless Sensor Network (WSN) where the sensors are mounted on the appliances and they are able to run web services. The web server retrieves data from the appliances via the web services running on the sensor nodes. These data can be stored in a database after processing, where the database can be accessed by the utility, as well as the inhabitants of the smart home. We show that our implementation is efficient in terms of running time. Moreover, the message sizes and the implementation code is quite small which makes it suitable for the memory-limited sensor nodes. Furthermore, we show the application scenarios introduced in the paper provide energy saving for the smart home. Smart Grid is aimed to incorporate monitoring, analysis, control and communication capabilities to improve reliability and energy efficiency. However, currently there is no enough sensor to provide



information interface for the implementation of smart grid. Therefore, new types of sensors should be deployed to assist the implementation of smart grid. This paper proposes a novel scheme, in which new type of fiber optic sensors (as compared with traditional Farady effect based fiber optic sensor used in power system instrumentation) are used to provide multiple types of information for smart grid. The new Fiber Gragg Gratting (FBG) is advantageous in that it can collect variant types of information and can form a sensor network. A transmission line monitoring system with distributed fiber optic senor setwork is designed, and the procedures to evaluate the status of the overhead transmission line (such as sag, vibration, and galloping) are proposed. A testing setup is built at laboratory, and it is shown that the FBG sensor is capable of obtaining the comprehensive information for evaluating the status of the overhead transmission line.

A. Converger fiber wireless access networks

Converged fiber-wireless (FiWi) access networks may be viewed as the endgame of broadband access. They hold promise to replace commuting with teleworking, which, taking the United States as an example, could lead to dramatic savings of 136 billion vehicle travel miles annually in the US by 2020 and 171 billion miles by 2030 [1]. At the downside, FiWi networks and access networks in general suffer from a major shortcoming. In today's Internet, the total energy consumption is dominated by access networks and as access rates of tens of Mbit/s become commonplace, it will be necessary to improve their energy efficiency in order to avoid a significantly increased greenhouse footprint of the Internet [2]. Previous work on "green" communications networks focused only on the reduction of their own energy consumption and greenhouse gas emissions. It is only recently that research has begun to study the role of green access networks and adopt them also in other relevant sectors to enhance the efficiency of energy use, resulting in a dramatically increased overall CO2 reduction across multiple economic sectors [3]. In this paper, we explore the opportunities and challenges of enhancing FiWi broadband access networks with fiber optic and wireless sensors and adopting the resultant fiberwireless sensor networks (Fi-WSNs) to convert the traditional electric power grid, the largest mancreated CO2 emission source, into the future smart grid. Today's power networks have to increase their utilization and become more efficient without depleting our ever declining natural resources to meet the increasing electricity demand of a rapidly growing global population from 6.1 billion in 2000 to 7.5 billion by 2020, leading to a staggering 75% increase in power consumption by 2020. Toward this end, the current power grid has to be transformed

into the smart grid by incorporating sophisticated sensing, monitoring, information, and communications technologies to provide better grid performance and support a wide range of additional services to consumers. The remainder of the paper is structured as follows. Section 2 briefly reviews the vision of smart grid and elaborates on its anticipated benefits and possible pitfalls. In Section 3, we propose a Fi-WSN based smart grid communications infrastructure and elaborate on is implementation models.

In the literature, demand management have been studied in several works. In [10], the authors propose cycling on and off refrigerators for frequency regulation services. The European SMART-A project discusses delaying the cycles of appliances according to the local power generation capacity of a house [11]. Aggregated residential demand response programs have also been considered in [12]. A residential load control (RLC) scheme that is suitable for grids with real-time pricing is proposed in [4]. The authors focus on an automatic controller that is able to predict the price of electricity during the scheduling horizon and schedule appliances to provide an optimum cost and waiting time within that horizon. Our optimization based solution is different than [4], as in our scheme, consumers can choose an upper limit for the waiting time at the setup time and we make use of TOU rates and exploit communications. In [5], the authors propose a decision-support tool (DsT) for smart homes. A PHEV, space heater, water heater, pool pump, and a PV system are scheduled based on various TOU tariffs by using the particle swarm optimization technique. In [5], the communication among the distributed resources and consumers has not been considered, whereas in our scheme, the controller and the users communicate through appliance interfaces. In [6], several management and control schemes are proposed for microgrids and for single houses. The authors use a neural networkbased prediction approach to predict the day-ahead demand. According to the predicted demand, the schedule of the microCHP device in each house is optimized. In addition, local appliances are controlled to optimize electricity import/export of the home. Our optimization-based residential energy management is different than [6] since we aim to minimize the cost of electricity based on TOU rates. Our work relies on demand shifting rather than scheduling generation and consumption to attain a balance. Moreover, in our paper, we assume that each house makes independent decisions unlike a set of houses being controlled by a steering signal from a global controller as described in [6]. In [7], the authors focus on reducing the peak-to-average electricity usage ratio by finding an optimal consumption schedule (OCS) for the subscribers in a neighborhood. The authors employ a game theoretic



approach. In [13], the authors propose an energy management protocol which allows consumers to set a maximum consumption value and the residential gateway is able to turn off the appliances that are in standby mode, or overwriting the user defined programmes with lessenergy consuming ones. However, defining a maximum value

II. OPTIMIZATION BASED RESIDENTIAL ENERGY MANAGEMENT (OREM)

We propose an LP model to minimize the total cost of electricity usage at home. Despite that home appliances consume the same amount of energy regardless of the time they are switched on, in the smart grid, as a result of the TOU tariffs, the hours when the appliances are used affect the cost of energy. In the OREM scheme, we assume that one day is divided into equal length consecutive timeslots which have varying prices for electricity consumption similar to TOU tariff. Our objective function minimizes the total energy expenses by scheduling the appliances in the appropriate timeslots. In the LP model, consumer requests are given as an input and an optimum scheduling is achieved at the output. In this application, the information is provided by the Schneider Electric Smart meter PM800, Figure 2, which has several capabilities that include:

• Power quality compliance monitoring Validate that power delivered or received complies with the EN50160 international power quality standard.

• Disturbance and harmonic analysis Detect, troubleshoot and resolve power anomalies that can affect sensitive manufacturing, production, data or laboratory processes and equipment.

• Energy metering, cost allocation and subbilling Upload metered energy values to software to support utility bill verification, contract optimization and cost allocation or billing by department, area or process.

• Demand and power factor control Trend and forecast energy and demand to help analyze usage patterns, compare load characteristics and manage energy costs. Manage demand or power factor using set point-triggered relays to control loads or capacitor banks.

• Load studies and circuit optimization Optimize load curtailment and load preservation programs to drive down energy costs and improve system reliability. Reveal unused electrical system capacity.

• Equipment monitoring and control Monitor the status or condition of breakers, generators or other equipment. Automatically or manually control equipment using on-board relays.

• Preventive maintenance Track and alarm on equipment conditions that could indicate excessive wear, imminent malfunction or poor energy inefficiency. Verify that power distribution and mitigation equipment is operating reliably and within specified tolerances. • Integrated utility metering

ACORD is a home appliance coordination scheme for the smart grid. ACORD allows for flexible start times for home appliances. In the ACORD scheme, the consumer turns on the appliance at any time regardless of peak hour concern. This consumer request generates a START-REQ packet. The START-REQ packet contains the duration of the cycle of the appliance. This could be a washing cycle for a washer or the time required for the coffee maker to make the desired amount of coffee. START-REO packet is sent to the EMU by wireless communication. Wireless communication may experience loss of connectivity due to obstructions such as walls or inhabitants. In a large house, EMU may be physically far from appliances. This means the EMU may not be within the reach of all appliances at one hop and multiple hops may be required for message delivery. In this case, an already deployed home area sensor network can be used to relay packets of the appliances. The sensor network can continue to work for its deployment purpose, such as inhabitant health monitoring or air conditioning for each individual inhabitant and at the same time it can relay energy management messages. Using a sensor network alleviates the need for A2A communication. A2A communication is challenging because appliance vendors may employ different standards which has been the common practice in the industry. EMU receives the START-REQ packet and schedules an available start time. It can also communicate with the smart meter and update the TOU rate and peak hour information. The EMU computes the waiting time as the difference between the next available start time and the consumer desired start time. The waiting time is sent by START-REP packet. EMU determines the waiting time as follows. If the consumer desired start time in the START-REQ packet is in off-peak hours and there is no earlier request on that time, the waiting time is set to zero. If there has been earlier requests, EMU schedules the new request at the end of the previous request. EMU avoids to schedule start times in the peak hours. When the user desired start time or the scheduled start time falls between peak hours, they are shifted to off peak hours. EMU also avoids shifting appliance cycles to the next days to prevent bursty loads. The waiting time information is sent to the consumer for approval in the START-REP packet. The consumer may be willing to negotiate with the EMU and wait for some time. In this case, the consumer will benefit from lower energy bills. On the other hand, the consumer may need to start the appliance immediately. The decision is up to the consumer, EMUdoes not force a start time on the appliances because this could cause discomfort on the consumer side. The decision of the consumer is sent back to EMU in the NOTIFICATION packet. EMU uses the consumer

ONLINE PEER REVIEWED JOURNAL International Journal of Computational Engineering Research

decision to reserve a time slot for the appliance and use this reserved time information for the scheduling of future requests.

A. IEEE 802.15.4 based WSN

The IEEE 802.15.4 [11] refers to the first two layers of the ISO/OSI stack protocol, i.e. the standard defines the physical layer (PHY) and medium access control (MAC) sub-layer specifications for supporting simple devices that consume minimal power and typically operate in the wireless personal area network (WPAN) of 10 m or in general in a short communication range. IEEE 802.15.4 is a standard for PAN which is also characterized by low data rate and low cost. In IEEE 802.15.4, all devices are divided into two categories: full function devices (FFDs) and refined function devices (RFDs) according to their capabilities. FFDs can initiate a WPAN and act as the coordinator of the WPAN, or can forward data and act as routers. At the physical layer, wireless links under 802.15.4 can operate in three license free industrial scientific medical (ISM) frequency bands. These accommodate over air data rates of 250 kbps in the 2.4 GHz band, 40 kbps in the 915 MHz band, and 20 kbps in the 868 MHz. A total of 27 channels are allocated in 802.15.4, including 16 channels in the 2.4 GHz band, available worldwide, 10 channels in the 915 MHz band, used in North America, and 1 channel in the 868 MHz band for Europe. Many technologies based on the IEEE 802.15.4 standard have been deployed for WPANs. Among these, the ZigBee appears particularly suitable for the applicative domain under study. The ZigBee has been well accepted as industrial standard for wireless sensor networks because it allows good achievements in many application domains (i.e. environment monitoring, home network, industrial automation). ZigBee adopts IEEE 802.15.4 standard at its PHY and MAC layers and support lowrate WPANs. Its specifications add to the standard four main components: network layer, application layer, ZigBee device objects (ZDOs) and userdefined application objects which allows for customization and flexibility within the standard. At its core, ZigBee is a mesh network architecture. Its network layer natively supports as main topologies: star and tree typical networks and generic mesh networks, self-forming and self-healing networks. In particular, the ZigBee architecture identifies three kinds of devices:

- A coordinator, which organizes the sensor network and maintains routing tables.

- Routers, which can talk to the coordinator, to other routers and to reduced-function end devices.

- End devices, which can talk to routers and the coordinator, but not to each other.

The expected benefits deriving by the application of this communication architecture are:

- Low cost: a typical ZigBee modem can be as low as \$12 each in quantities as few as 100 pieces.

This pricing provides an economic justification for extending wireless networking to even the simplest of devices.

- Range and obstruction issues avoidance: the routers double as input devices and repeaters, to create a form of mesh network. In this way, if two network points are unable to communicate as intended, transmission is dynamically routed from the blocked node to a router with a clear path to the data's destination. This happens automatically, so that communications continue even when a link fails unexpectedly. The use of low-cost routers can also extend the network's effective reach. When the distance between the base station and a remote node exceeds the devices' range, an intermediate node or nodes can relay transmission, eliminating the need for separate repeaters without stopping the system operation. This long-term reliability is critical for many power automation systems that are expected to last 20-30 years once installed.

B. Residential energy management

Residential energy management has been neglected in the exiting power grid due to scalability concerns. However, in the smart grid, ICT technologies enable energy management for each individual residential unit. Utilities may remotely apply energy management in order to intentionally reduce peak load. This is generally meaningful when the grid faces a risk of failure but even though there is no failure risk, reducing the peak load is important because it results in less emissions and less expenses. For this reason, consumers may willingly reduce their peak consumption by the use of energy management schemes. In our residential energy management application, communication among the appliances and the energy manager uses Zigbee with short-range wireless links. Zigbee is a lowdata rate, short-range, energy-efficient wireless technology that is based on the IEEE 802.15.4 standard. It utilizes 16 channels in the 2.4GHz ISM band worldwide, 13 channels in the 915MHz band in North America and one channel in the 868MHz band in Europe and it can support data rates of 250 kbps, 100kbps (available in IEEE 802.15.4-2006), 40 kbps, and 20 kbps. Zigbee provides low power consumption due to its low duty cycle mechanism. Residential energy management scheme works as follows. When a consumer turns on an appliance, the appliance communicates with the energy manager by sending a STARTREQ packet. This packet contains the sequence number of the request, request generation time and the duration the appliance cycle. Energy manager computes a convenient start time for the appliance by considering the availability of the local energy generation and the price of electricity. The time interval between the convenient start time and the consumer requested start time is



called the waiting time. If the waiting time is above a threshold Wmax, then the appliance is started immediately to prevent accumulating the requests on one day. The waiting time is sent back to the appliance in a START-REP packet and it is displayed to the consumer via an LCD. The consumer may be willing to negotiate and wait for some time or she may need to start the appliance immediately. The energy manager does not force an automated start time because this could cause discomfort on the consumer side. Consumer decision is sent back to the energy manager in a NOTIFICATION packet. The algorithm for determining the waiting time is given in Algorithm 1. If the consumer requested start time is in peak periods, the energy manager checks the availability of the local energy source, and if it is available then the waiting time is set to zero. When there is not enough local energy, the suggested start time is shifted to off peak hours. The packets of the energy management application is relayed by the WSHAN. The distance between the appliances and the energy manager may exceed the length of the Zigbee links and multiple hops may be required. Moreover construction type or interference on a link may necessitate multiple hops. In this case, the existing WSHAN in the smart home that has been initially set up for inhabitant health monitoring, air conditioning, etc, can be used to relay the packets of the energy management application.

C. Key design aspects

Radio Design: An 802.15.4 radio in ZigBee pro stack currently supports receiver sensitivity up to -100 dbm [3].

However to make it cognitive we require higher receiver sensitivity up to -114dbm as per the FCC regulation. The radio needs to operate across wide band to cover licensed bands. Reference [7] suggests several methods to do so. Also, a very crucial decision we need to make is about selecting dual or single radio architecture. As explained earlier updating channel back up list can be carried out independently without having quiet periods if we have dual antennas.

Spectrum Sensor Selection: White space or PU activity detection depends on three key parameters: Time, frequency and location [8]. Physical layer enables us to create opportunity in time and frequency naturally. With the help of network layer, we can exploit the location dimension as well. Therefore we select multiple spectrum sensors across the network. A device when it joins the network automatically chooses to become a spectrum sensor devices or coordinator. DIO from spectrum sensor devices or coordinator. DIO stands for DAG Information Objects and DAG stands for Directed Acyclic Graph. Both DAG and DIO are to be discussed in detail in section III. If the device listens to DIO, then it would just be a non-

spectrum sensing node. However we need to keep in mind an important fact that the spectrum sensor selection always should happen while operating in a ZigBee channel, since usually in PU channels all devices would be in each other's listening range and spectrum sensor selection logic would fail.

D. Conditions to change the incumbent channel

Frequency Agility (Channel Change): ZigBee pro stack has a dedicated network channel manager, usually the coordinator, which receives interference reports from other routers in the network. These routers keep track of failure counts. If the packet delivery success rate falls below 25% for 20 or greater messages transmitted by a node, then the node reports it to the networkmanager. Later, if the network manager decides to change channel it issues a notification to indicate the channel change [3].

Opening Joining Window: The coordinator needs to send a permit-join-request to all the routing capable devices in the network with a finite window period [3], during which, the network can add a new device. Whenever this happens all the nodes in the network need to move to a ZigBee channel picked from the common back up list and need to add the new device in that channel. If we do not have any ZigBee channel in our list, then we cannot add the new device. If the lists are not synchronized, the device with obsolete list would not participate in the joining process and soon after it realizes that it is on a wrong channel, it comes back to the previous channel. If network is still not established, the lost device needs to initiate a silent rejoin procedure which shall be discussed later.

Primary User (PU) Detection: When a strong signal from PU arrives, then the whole communication would be disrupted and all the devices get into receive mode and moves to the next channel as per the backup list in its data base. When a weak PU is expected to be detected, it is similar as explained in the quiet period section.

Channel Occupation Time Expiry: If none of the above scenarios (strong or weak PU detection) occurs then automatically the channel change takes place after COT=30 sec (see Table I) while operating in licensed band.

F. Joining procedures:

Normal Join/ New Device Join: A new device not belonging to any network sends beacon request and wait for beacons indicating that the network is accepting new association requests. It iterates this procedure across all 16 ZigBee channels until it joins a network. Now, when joining window opening is indicated by any coordinator, then all the devices currently in the network respond to the beacon requests by sending beacons. Say while a user enters security code on the Coordinator communication module, all the existing devices in the network move to a common ZigBee channel picked from their channel back up list and they reply by sending beacons to new device beacon requests. Later if the new device joins the network after being validated, it calculates its DIO and then it sends a device announcement. It is a unicast message to the coordinator. When the announcement reaches the coordinator, the devices through the path would record the new device entry in their routing table according to the routing path [2]. A new device cannot enter licensed channels directly. Since their beacon requests can cause interference to the PU. Also the newly joined device needs to receive the current time, next quite period initiation time and serial number from the coordinator to ensure synchronization.

🕼 IJCER

Silent Join/ Rejoin: This kind of join occurs for a device which remembers its network credentials. It happens when a device wakes after sleeping or when it was powered off or when it goes out of range. The sleeping device or unplugged device directly gets into the receive mode and waits in the present channel for a finite time and later if it does not listen to any packets from its own network, it listens across all the channels on the back up list serially, until it sniffs a packet from its current network. A device out of range after a threshold number of retransmissions, tries to find a new parent by broadcasting a DIO request to its neighbors. If it still does not receive any DIOs it should get into receive mode and acts like a woken up sleepy device as explained above.

III. NETWORK LAYER DESIGN FOR CR-WSN A. The RPL framework

The key idea of RPL is to maintain network state information using one or more DAGs. A DAG is a directed graph wherein all edges are oriented in such a way that no loops exist. For each DAG created in RPL, there is a root. The DAG root typically is the coordinator in smart grid utility networks. Each node in the DAG is associated with a rank value. The rank of nodes along any path to the DAG root should be monotonically decreasing in order to avoid any routing loop. In order to construct a DAG, the gateway node will issue a DIO [4].

B. Packet forwarding rules

Node to Coordinator (Forward Path): A meter node that generates or receives a data packet destined to the coordinator should forward this packet to its default parent. The packet should be dropped if the node does not have a default parent.

Coordinator to Node (Reverse Path): A node that generates or receives a data packet destined to node "i" should search for i's entry

inside the destination list (DL), if found forward the packet to the next-hop node indicated as per the list, else the packet should be dropped.

C. Network info tuples contained by different node types

- Node ID: Each node in the network is uniquely identified by its node ID i.e. IP address of the node.
- DAG ID: Node ID of the coordinator.
- Node Type: Coordinator /Spectrum Sensor/ ordinary node.
- Rank: This explains its distance from the PAN coordinator.
- Neighbor list: It's a list of neighbor entries. It contains the entries of all the nodes in the network to which it can
- listen. Following are the parameters corresponding to each neighbor list entry: The node ID of the neighbor node, Rank of the corresponding neighbor node, The ETX of the link from current node to corresponding neighbor node.
- Default Parent ID: It is the node ID of the neighbor node with the least rank in the neighbor list.
- Destination list (DL): It is nothing but a routing table. It consists of following parameters associated with each
- entry: The ID of the destination node, ID of the next hop node.
- Spectrum Sensor list: This consists of the entire node IDs of elected Spectrum Sensor nodes.
- Channel Backup list: This contains the frequency bands list with their priorities.
- PA or Non-PA: Contains power amplifier or not while transmitting.
- BD or Non-BD: A node is battery driven or not.

Ordinary node (neither coordinator/spectrum sensor):

(DAG ID, Node ID, Node Type, Rank, Neighbor list, Default parent ID, DL, PA or Non-PA, BD or Non-BD, Channel backup list)

Coordinator: (DAG ID, Node ID, Node Type, Rank, Neighbor list, Default parent ID, DL, PA or Non-PA, BD or

Non-BD, Channel backup list, Spectrum Sensor list)

Spectrum Sensor: (DAG ID, Node ID, Node Type, Rank, Neighbor list, Default parent ID, DL, PA or Non-PA, BD or Non-BD, Channel backup list). An ordinary node can hear DIOs from more than one Spectrum Sensors but no Spectrum Sensor would hear a DIO from another Spectrum Sensor.

We consider the following anycast field equations defined over an open bounded piece of network and /or feature space $\Omega \subset \mathbb{R}^d$. They describe the

dynamics of the mean anycast of each of p node populations.

🕼 IJCER

$$\begin{cases} (\frac{d}{dt}+l_{i})V_{i}(t,r) = \sum_{j=1}^{p} \int_{\Omega} J_{ij}(r,\bar{r})S[(V_{j}(t-\tau_{ij}(r,\bar{r}),\bar{r})-h_{|j})]d\bar{r} \\ + I_{i}^{ext}(r,t), \quad t \ge 0, 1 \le i \le p, \\ V_{i}(t,r) = \phi_{i}(t,r) \quad t \in [-T,0] \end{cases}$$
(1)

We give an interpretation of the various parameters and functions that appear in (1), Ω is finite piece of nodes and/or feature space and is represented as an open bounded set of \mathbb{R}^d . The vector r and \bar{r} represent points in Ω . The function $S: \mathbb{R} \to (0,1)$ is the normalized sigmoid function:

$$S(z) = \frac{1}{1 + e^{-z}}$$
(2)

It describes the relation between the input rate V_i of population *i* as a function of the packets potential, for example, $V_i = v_i = S[\sigma_i(V_i - h_i)].$ We note V the p- dimensional vector (V_1, \dots, V_p) . The *p* function $\phi_i, i = 1, \dots, p$, represent the initial conditions, see below. We note ϕ the p - dimensional vector $(\phi_1, ..., \phi_n)$. The p function $I_i^{ext}, i = 1, ..., p$, represent external factors from other network areas. We note I^{ext} the p - dimensional vector $(I_1^{ext}, ..., I_p^{ext})$. The $p \times p$ matrix of functions $J = \{J_{ij}\}_{i, j=1,...,p}$ represents the connectivity between populations i and j, see below. The *p* real values $h_i, i = 1, ..., p_i$ determine the threshold of activity for each population, that is, the value of the nodes potential corresponding to 50% of the maximal activity. The p real positive values σ_i , i = 1, ..., p, determine the slopes of the sigmoids at the origin. Finally the p real positive values l_i , i = 1, ..., p, determine the speed at which each anycast node potential decreases exponentially toward its real value. We also introduce the function $S: \mathbb{R}^p \to \mathbb{R}^p$, defined $S(x) = [S(\sigma_1(x_1 - h_1)), ..., S(\sigma_p - h_p))],$ by diagonal and the $p \times p$ matrix $L_0 = diag(l_1, ..., l_p)$. Is the intrinsic dynamics of the population given by the linear response of data transfer. $(\frac{d}{dt} + l_i)$ is replaced by $(\frac{d}{dt} + l_i)^2$ to use the alpha function response. We use $(\frac{d}{d_i} + l_i)$ for simplicity although our analysis applies to more general intrinsic dynamics. For the sake, of generality, the propagation delays are not assumed to be identical for all populations, hence they are described by a matrix $\tau(r,r)$ whose element $au_{ii}(r,r)$ is the propagation delay between population j at r and population i at r. The reason for this assumption is that it is still unclear from anycast if propagation delays are independent of the populations. We assume for technical reasons that τ is continuous, that is $\tau \in C^0(\overline{\Omega}^2, R_+^{p \times p})$. Moreover packet data indicate that τ is not a symmetric function i.e., $\tau_{ii}(r, r) \neq \tau_{ii}(r, r)$, thus no assumption is made about this symmetry unless otherwise stated. In order to compute the righthand side of (1), we need to know the node potential factor V on interval [-T, 0]. The value of T is obtained by considering the maximal delay:

$$\tau_m = \max_{i,j(r,\bar{r}\in\overline{\Omega\times\Omega})} \tau_{i,j}(r,\bar{r})$$
(3)

Hence we choose $T = \tau_m$

D. Mathematical Framework

A convenient functional setting for the nondelayed packet field equations is to use the space $F = L^2(\Omega, \mathbb{R}^p)$ which is a Hilbert space endowed with the usual inner product:

$$\left\langle V, U \right\rangle_F = \sum_{i=1}^p \int_{\Omega} V_i(r) U_i(r) dr$$
 (1)

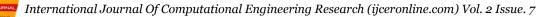
To give a meaning to (1), we defined the history space $C = C^0([-\tau_m, 0], F)$ with $\|\phi\| = \sup_{t \in [-\tau_m, 0]} \|\phi(t)\| F$, which is the Banach phase space associated with equation (3). Using the notation $V_t(\theta) = V(t + \theta), \theta \in [-\tau_m, 0]$, we write (1) as

$$\begin{cases} V(t) = -L_0 V(t) + L_1 S(V_t) + I^{ext}(t), \\ V_0 = \phi \in C, \end{cases}$$
(2)

Where

$$\begin{cases} L_1: C \to F, \\ \phi \to \int_{\Omega} J(., \bar{r}) \phi(\bar{r}, -\tau(., \bar{r})) d\bar{r} \end{cases}$$

Is the linear continuous operator satisfying $\|L_1\| \leq \|J\|_{L^2(\Omega^2, R^{p \times p})}$. Notice that most of the



papers on this subject assume Ω infinite, hence requiring $\tau_m = \infty$.

Proposition 1.0 If the following assumptions are satisfied.

1.
$$J \in L^2(\Omega^2, \mathbb{R}^{p \times p}),$$

2. The external current
$$I^{ext} \in C^0(R, F)$$
,

3.
$$\tau \in C^0(\Omega^2, R^{p \times p}_+), \sup_{\overline{\Omega^2}} \tau \leq \tau_m$$

Then for any $\phi \in C$, there exists a unique solution

$$V \in C^{1}([0,\infty), F) \cap C^{0}([-\tau_{m},\infty, F) \text{ to } (3)$$

Notice that this result gives existence on R_+ , finitetime explosion is impossible for this delayed differential equation. Nevertheless, a particular solution could grow indefinitely, we now prove that this cannot happen.

E. Boundedness of Solutions

A valid model of neural networks should only feature bounded packet node potentials.

Theorem 1.0 All the trajectories are ultimately bounded by the same constant R if $I \equiv \max_{t \in R^+} \|I^{ext}(t)\|_{E} < \infty.$

Proof :Let us defined $f: R \times C \rightarrow R^+$ as

$$f(t,V_t) \stackrel{def}{=} \left\langle -L_0 V_t(0) + L_1 S(V_t) + I^{ext}(t), V(t) \right\rangle_F = \frac{1}{2} \frac{d \left\| V \right\|_F^2}{dt}$$

We note $l = \min_{i=1,\dots,p} l_i$

$$f(t,V_t) \le -l \|V(t)\|_F^2 + (\sqrt{p|\Omega|} \|J\|_F + I) \|V(t)\|_F$$

Thus, if

$$\|V(t)\|_{F} \ge 2 \frac{\sqrt{p|\Omega|} \|J\|_{F} + I}{l} \stackrel{\text{def}}{=} R, f(t, V_{t}) \le -\frac{lR^{2}}{2} \stackrel{\text{def}}{=} -\delta < 0$$

Let us show that the open route of F of center 0 and radius R, B_R , is stable under the dynamics of equation. We know that V(t) is defined for all $t \ge 0s$ and that f < 0 on ∂B_R , the boundary of B_R . We consider three cases for the initial condition V_0 . If $\|V_0\|_c < R$ and set $T = \sup\{t \mid \forall s \in [0, t], V(s) \in B_{\mathbb{R}}\}.$ Suppose that $T \in \mathbb{R}$, then V(T) is defined and belongs to B_R , the closure of B_R , because B_R is closed, in ∂B_R , effect we also to have

$$\frac{d}{dt} \left\| V \right\|_F^2 |_{t=T} = f(T, V_T) \le -\delta < 0 \qquad \text{because}$$

 $V(T) \in \partial B_R$. Thus we deduce that for $\varepsilon > 0$ and small enough, $V(T+\varepsilon) \in \overline{B_R}$ which contradicts the definition of T. Thus $T \notin R$ and $\overline{B_R}$ is stable.

Because f<0 on $\partial B_R, V(0) \in \partial B_R$ implies that $\forall t > 0, V(t) \in B_R$. Finally we consider the case $V(0) \in \overline{CB_R}$. Suppose that $\forall t > 0, V(t) \notin \overline{B_R}$, then

$$\forall t > 0, \frac{d}{dt} \|V\|_F^2 \le -2\delta$$
, thus $\|V(t)\|_F$ is

monotonically decreasing and reaches the value of R in finite time when V(t) reaches ∂B_R . This contradicts our assumption. Thus $\exists T > 0 | V(T) \in B_R$.

Proposition 1.1 : Let *s* and *t* be measured simple functions on X. for $E \in M$, define

$$\phi(E) = \int_{E} s \, d\mu \qquad (1)$$

Then ϕ is a measure on M .
$$\int_{X} (s+t) d\mu = \int_{X} s \, d\mu + \int_{X} t d\mu \qquad (2)$$

Proof: If s and if $E_1, E_2, ...$ are disjoint members of M whose union is E, the countable additivity of μ shows that

$$\phi(E) = \sum_{i=1}^{n} \alpha_i \mu(A_i \cap E) = \sum_{i=1}^{n} \alpha_i \sum_{r=1}^{\infty} \mu(A_i \cap E_r)$$
$$= \sum_{r=1}^{\infty} \sum_{i=1}^{n} \alpha_i \mu(A_i \cap E_r) = \sum_{r=1}^{\infty} \phi(E_r)$$

Also, $\varphi(\phi) = 0$, so that φ is not identically ∞ . Next, let *s* be as before, let $\beta_1, ..., \beta_m$ be the distinct values of t, and let $B_j = \{x : t(x) = \beta_j\}$ If $E_{ij} = A_i \cap B_j$, the $\int_{E_{ij}} (s+t)d\mu = (\alpha_i + \beta_j)\mu(E_{ij})$ and $\int_{E_{ij}} sd\mu + \int_{E_{ij}} td\mu = \alpha_i\mu(E_{ij}) + \beta_j\mu(E_{ij})$ Thus (2) holds with E_{ij} in place of *X*. Since *X* is

the disjoint union of the sets E_{ij} $(1 \le i \le n, 1 \le j \le m)$, the first half of our proposition implies that (2) holds.



Theorem 1.1: If K is a compact set in the plane whose complement is connected, if f is a continuous complex function on K which is holomorphic in the interior of , and if $\varepsilon > 0$, then there exists a polynomial P such that $|f(z) = P(z)| < \varepsilon$ for all $z \varepsilon K$. If the interior of K is empty, then part of the hypothesis is vacuously satisfied, and the conclusion holds for every $f \varepsilon C(K)$. Note that K need to be connected. *Proof:* By Tietze's theorem, f can be extended to a

Proof: By Letze's theorem, f can be extended to a continuous function in the plane, with compact support. We fix one such extension and denote it again by f. For any $\delta > 0$, let $\omega(\delta)$ be the supremum of the numbers $|f(z_2) - f(z_1)|$ Where z_1 and z_2 are subject to the condition $|z_2 - z_1| \le \delta$. Since f is uniformly continous, we have $\lim_{\delta \to 0} \omega(\delta) = 0$ (1) From now on, δ will be fixed. We shall prove that there is a

 δ will be fixed. We shall prove that there is a polynomial P such that

$$|f(z) - P(z)| < 10,000 \ \omega(\delta) \ (z \in K)$$
 (2)

By (1), this proves the theorem. Our first objective is the construction of a function $\Phi \varepsilon C_c(R^2)$, such that for all *z*

$$\begin{split} \left| f(z) - \Phi(z) \right| &\leq \omega(\delta), \quad (3) \\ \left| (\partial \Phi)(z) \right| &< \frac{2\omega(\delta)}{\delta}, \quad (4) \end{split}$$

And

$$\Phi(z) = -\frac{1}{\pi} \iint_{X} \frac{(\partial \Phi)(\zeta)}{\zeta - z} d\zeta d\eta \qquad (\zeta = \xi + i\eta), \qquad (5)$$

Where X is the set of all points in the support of Φ whose distance from the complement of K does not δ . (Thus X contains no point which is "far within" K.) We construct Φ as the convolution of f with a smoothing function A. Put a(r) = 0 if $r > \delta$, put

$$a(r) = \frac{3}{\pi\delta^2} (1 - \frac{r^2}{\delta^2})^2 \qquad (0 \le r \le \delta), \quad (6)$$

And define

$$A(z) = a(|z|) \tag{7}$$

For all complex z. It is clear that $A \varepsilon C'_c(R^2)$. We claim that

$$\iint_{R^{s}} A = 1, \qquad (8)$$

$$\iint_{R^{2}} \partial A = 0, \qquad (9)$$

$$\iint_{R^{3}} |\partial A| = \frac{24}{15\delta} < \frac{2}{\delta}, \qquad (10)$$

The constants are so adjusted in (6) that (8) holds. (Compute the integral in polar coordinates), (9) holds simply because A has compact support. To compute (10), express ∂A in polar coordinates, and note that $\partial A / \partial \theta = 0$,

$$\partial A / \partial r = -a',$$

Now define

$$\Phi(z) = \iint_{R^2} f(z-\zeta) A d\xi d\eta = \iint_{R^2} A(z-\zeta) f(\zeta) d\xi d\eta \qquad (11)$$

Since f and A have compact support, so does Φ . Since

$$\Phi(z) - f(z)$$

$$= \iint_{R^2} [f(z - \zeta) - f(z)] A(\xi) d\xi d\eta \quad (12)$$

And $A(\zeta) = 0$ if $|\zeta| > \delta$, (3) follows from (8). The difference quotients of A converge boundedly to the corresponding partial derivatives, since $A \varepsilon C'_c(R^2)$. Hence the last expression in (11) may be differentiated under the integral sign, and we obtain

$$(\partial \Phi)(z) = \iint_{R^2} (\overline{\partial A})(z - \zeta) f(\zeta) d\xi d\eta$$

$$= \iint_{R^2} f(z - \zeta) (\partial A)(\zeta) d\xi d\eta$$

$$= \iint_{R^2} [f(z - \zeta) - f(z)](\partial A)(\zeta) d\xi d\eta \qquad (13)$$

The last equality depends on (9). Now (10) and (13) give (4). If we write (13) with Φ_x and Φ_y in place of $\partial \Phi$, we see that Φ has continuous partial derivatives, if we can show that $\partial \Phi = 0$ in *G*, where *G* is the set of all $z \in K$ whose distance from the complement of *K* exceeds δ . We shall do this by showing that $\Phi(z) = f(z)$ ($z \in G$): (14)

$$\Phi(z) = f(z) \quad (z \in G);$$
(14)
Note that $\partial f = 0$ in G, since f is holomorphic
there. Now if $z \in G$, then $z - \zeta$ is in the interior of



K for all ζ with $|\zeta| < \delta$. The mean value property for harmonic functions therefore gives, by the first equation in (11),

$$\Phi(z) = \int_{0}^{\delta} a(r)rdr \int_{0}^{2\pi} f(z - re^{i\theta})d\theta$$

= $2\pi f(z) \int_{0}^{\delta} a(r)rdr = f(z) \iint_{R^{2}} A = f(z)$ (15)

For all $z \in G$, we have now proved (3), (4), and (5) The definition of X shows that X is compact and that X can be covered by finitely many open discs $D_1, ..., D_n$, of radius 2δ , whose centers are not in K. Since $S^2 - K$ is connected, the center of each D_j can be joined to ∞ by a polygonal path in $S^2 - K$. It follows that each D_j contains a compact connected set E_j , of diameter at least 2δ , so that $S^2 - E_j$ is connected and so that $K \cap E_j = \phi$. with $r = 2\delta$. There are functions $g_j \in H(S^2 - E_j)$ and constants b_j so that the inequalities.

$$\left| \mathcal{Q}_{j}(\zeta, z) \right| < \frac{50}{\delta}, \quad (16)$$

$$\left| \mathcal{Q}_{j}(\zeta, z) - \frac{1}{z - \zeta} \right| < \frac{4,000\delta^{2}}{\left| z - \zeta \right|^{2}} \quad (17)$$

Hold for $z \notin E_i$ and $\zeta \in D_i$, if

$$Q_{j}(\zeta, z) = g_{j}(z) + (\zeta - b_{j})g_{j}^{2}(z)$$
(18)

Let Ω be the complement of $E_1 \cup ... \cup E_n$. Then Ω is an open set which contains K. Put $X_1 = X \cap D_1$ and

$$X_{j} = (X \cap D_{j}) - (X_{1} \cup ... \cup X_{j-1}),$$
 for

 $2 \le j \le n$, Define

$$R(\zeta, z) = Q_j(\zeta, z) \qquad (\zeta \varepsilon X_j, z \varepsilon \Omega)$$
(19)
And

$$F(z) = \frac{1}{\pi} \iint_{X} (\partial \Phi)(\zeta) R(\zeta, z) d\zeta d\eta \qquad (20)$$
$$(z \in \Omega)$$

Since,

$$F(z) = \sum_{j=1}^{\infty} \frac{1}{\pi} \iint_{X_i} (\partial \Phi)(\zeta) Q_j(\zeta, z) d\xi d\eta, \qquad (21)$$

(18) shows that F is a finite linear combination of the functions g_j and g_j^2 . Hence $F \varepsilon H(\Omega)$. By (20), (4), and (5) we have

$$|F(z) - \Phi(z)| < \frac{2\omega(\delta)}{\pi\delta} \iint_{X} |R(\zeta, z)|$$
$$-\frac{1}{z - \zeta} |d\xi d\eta \quad (z \in \Omega) \quad (22)$$

Observe that the inequalities (16) and (17) are valid with R in place of Q_j if $\zeta \in X$ and $z \in \Omega$. Now fix $z \in \Omega$., put $\zeta = z + \rho e^{i\theta}$, and estimate the integrand in (22) by (16) if $\rho < 4\delta$, by (17) if $4\delta \le \rho$. The integral in (22) is then seen to be less than the sum of

$$2\pi \int_{0}^{4\delta} \left(\frac{50}{\delta} + \frac{1}{\rho}\right) \rho d\rho = 808\pi\delta$$
 (23)

And

$$2\pi \int_{4\delta}^{\infty} \frac{4,000\delta^2}{\rho^2} \rho d\rho = 2,000\pi\delta.$$
 (24)

Hence (22) yields

$$|F(z) - \Phi(z)| < 6,000 \omega(\delta)$$
 (z $\varepsilon \Omega$) (25)

Since $F \varepsilon H(\Omega)$, $K \subset \Omega$, and $S^2 - K$ is connected, Runge's theorem shows that F can be uniformly approximated on K by polynomials. Hence (3) and (25) show that (2) can be satisfied. This completes the proof.

Lemma 1.0 : Suppose $f \varepsilon C'_c(R^2)$, the space of all continuously differentiable functions in the plane, with compact support. Put

$$\partial = \frac{1}{2} \left(\frac{\partial}{\partial x} + i \frac{\partial}{\partial y} \right) \tag{1}$$

Then the following "Cauchy formula" holds:

$$f(z) = -\frac{1}{\pi} \iint_{R^2} \frac{(\partial f)(\zeta)}{\zeta - z} d\xi d\eta$$
$$(\zeta = \xi + in) \tag{2}$$

Proof: This may be deduced from Green's theorem. However, here is a simple direct proof:

Put
$$\varphi(r,\theta) = f(z + re^{i\theta}), r > 0, \theta$$
 real

If
$$\zeta = z + re^{i\theta}$$
, the chain rule gives

$$(\partial f)(\zeta) = \frac{1}{2}e^{i\theta} \left[\frac{\partial}{\partial r} + \frac{i}{r} \frac{\partial}{\partial \theta} \right] \varphi(r,\theta)$$
(3)

The right side of (2) is therefore equal to the limit, as $\mathcal{E} \rightarrow 0$, of

$$-\frac{1}{2}\int_{\varepsilon}^{\infty}\int_{0}^{2\pi} \left(\frac{\partial\varphi}{\partial r} + \frac{i}{r}\frac{\partial\varphi}{\partial\theta}\right) d\theta dr \qquad (4)$$

Issn 2250-3005(online)

November | 2012



For each $r > 0, \varphi$ is periodic in θ , with period 2π . The integral of $\partial \varphi / \partial \theta$ is therefore 0, and (4) becomes

$$-\frac{1}{2\pi}\int_{0}^{2\pi}d\theta\int_{\varepsilon}^{\infty}\frac{\partial\varphi}{\partial r}dr = \frac{1}{2\pi}\int_{0}^{2\pi}\varphi(\varepsilon,\theta)d\theta$$
(5)

As $\varepsilon \to 0$, $\varphi(\varepsilon, \theta) \to f(z)$ uniformly. This gives (2)

If $X^{\alpha} \in a$ and $X^{\beta} \in k[X_1,...X_n]$, then $X^{\alpha}X^{\beta} = X^{\alpha+\beta} \in a$, and so A satisfies the condition (*). Conversely,

$$(\sum_{\alpha \in A} c_{\alpha} X^{\alpha}) (\sum_{\beta \in \square^{n}} d_{\beta} X^{\beta}) = \sum_{\alpha, \beta} c_{\alpha} d_{\beta} X^{\alpha + \beta} \qquad (finite sums),$$

and so if A satisfies (*), then the subspace generated by the monomials $X^{\alpha}, \alpha \in a$, is an ideal. The proposition gives a classification of the monomial ideals in $k[X_1,...X_n]$: they are in one to one correspondence with the subsets A of \square^n satisfying (*). For example, the monomial ideals in k[X] are exactly the ideals $(X^n), n \ge 1$, and the zero ideal (corresponding to the empty set A). We write $\langle X^{\alpha} | \alpha \in A \rangle$ for the ideal corresponding to A (subspace generated by the $X^{\alpha}, \alpha \in a$).

LEMMA 1.1. Let S be a subset of \Box^n . The the ideal a generated by $X^{\alpha}, \alpha \in S$ is the monomial ideal corresponding to

 $A^{d_{f}}_{\underline{-}} \{ \beta \in \square^{n} \mid \beta - \alpha \in \square^{n}, \text{ some } \alpha \in S \}$

Thus, a monomial is in *a* if and only if it is divisible by one of the $X^{\alpha}, \alpha \in S$

PROOF. Clearly *A* satisfies (*), and $a \subset \langle X^{\beta} | \beta \in A \rangle$. Conversely, if $\beta \in A$, then $\beta - \alpha \in \square^{n}$ for some $\alpha \in S$, and $X^{\beta} = X^{\alpha} X^{\beta - \alpha} \in a$. The last statement follows from the fact that $X^{\alpha} | X^{\beta} \Leftrightarrow \beta - \alpha \in \square^{n}$. Let $A \subset \square^{n}$ satisfy (*). From the geometry of *A*, it is clear that there is a finite set of elements $S = \{\alpha_{1}, ... \alpha_{s}\}$ of *A* such that $A = \{\beta \in \square^{n} | \beta - \alpha_{i} \in \square^{2}, some \alpha_{i} \in S\}$ (The α_i 's are the corners of A) Moreover, $a \stackrel{df}{=} \langle X^{\alpha} | \alpha \in A \rangle$ is generated by the monomials $X^{\alpha_i}, \alpha_i \in S$.

DEFINITION 1.0. For a nonzero ideal a in $k[X_1,...,X_n]$, we let (LT(a)) be the ideal generated by $\{LT(f) | f \in a\}$

LEMMA 1.2 Let *a* be a nonzero ideal in $k[X_1,...,X_n]$; then (LT(a)) is a monomial ideal, and it equals $(LT(g_1),...,LT(g_n))$ for some $g_1,...,g_n \in a$.

PROOF. Since (LT(a)) can also be described as the ideal generated by the leading monomials (rather than the leading terms) of elements of a.

THEOREM 1.2. Every *ideal* a in $k[X_1,...,X_n]$ is finitely generated; more precisely, $a = (g_1,...,g_s)$ where $g_1,...,g_s$ are any elements of a whose leading terms generate LT(a)

PROOF. Let $f \in a$. On applying the division algorithm, find we $f = a_1g_1 + ... + a_sg_s + r, \qquad a_i, r \in k[X_1, ..., X_n]$, where either r = 0 or no monomial occurring in it $LT(g_i)$ divisible by any But is $r = f - \sum a_i g_i \in a$ and therefore , $LT(r) \in LT(a) = (LT(g_1), ..., LT(g_s))$ implies that every monomial occurring in r is divisible by one in $LT(g_i)$. Thus r=0, and $g \in (g_1, ..., g_s)$.

DEFINITION 1.1. A finite subset $S = \{g_1, | ..., g_s\}$ of an ideal a is a standard ((*Grobner*) bases for a if $(LT(g_1), ..., LT(g_s)) = LT(a)$. In other words, S is a standard basis if the leading term of every element of a is divisible by at least one of the leading terms of the g_i .

THEOREM 1.3 The ring $k[X_1,...,X_n]$ is Noetherian i.e., every ideal is finitely generated.



PROOF. For n = 1, k[X] is a principal ideal domain, which means that every ideal is generated by single element. We shall prove the theorem by induction on n. Note that the obvious map $k[X_1,...X_{n-1}][X_n] \rightarrow k[X_1,...X_n]$ is an isomorphism – this simply says that every polynomial f in n variables $X_1,...X_n$ can be expressed uniquely as a polynomial in X_n with coefficients in $k[X_1,...,X_n]$:

$$f(X_1,...X_n) = a_0(X_1,...X_{n-1})X_n^r + ... + a_r(X_1,...X_{n-1})$$

Thus the next lemma will complete the proof

LEMMA 1.3. If A is Noetherian, then so also is A[X]

PROOF. For a polynomial

$$f(X) = a_0 X^r + a_1 X^{r-1} + \dots + a_r, \quad a_i \in A, \quad a_0 \neq 0,$$

r is called the degree of f, and a_0 is its leading coefficient. We call 0 the leading coefficient of the polynomial 0. Let *a* be an ideal in A[X]. The leading coefficients of the polynomials in *a* form an ideal *a* in *A*, and since *A* is Noetherian, *a* will be finitely generated. Let g_1, \ldots, g_m be elements of *a* whose leading coefficients generate *a*, and let *r* be the maximum degree of g_i . Now let $f \in a$, and suppose *f* has degree s > r, say, $f = aX^s + \ldots$ Then $a \in a'$, and so we can write $a = \sum b_i a_i$, $b_i \in A$,

 $a_i = leading \ coefficient \ of \ g_i$ Now

 $f - \sum_{i} b_i g_i X^{s-r_i}$, $r_i = \deg(g_i)$, has degree $< \deg(f)$. By continuing in this way, we find that $f \equiv f_t \mod(g_1, \dots, g_m)$ With f_t а polynomial of degree t < r. For each d < r, let a_d be the subset of A consisting of 0 and the leading coefficients of all polynomials in a of degree d; it is again an ideal in A. Let $g_{d,1}, ..., g_{d,m_d}$ be polynomials of degree d whose leading coefficients generate a_d . Then the same argument as above shows that any polynomial f_d in a of d can written degree be $mod(g_{d,1},...,g_{d,m_d})$ With f_{d-1} $f_d \equiv f_{d-1}$

of degree $\leq d-1$. On applying this remark repeatedly we find that $f_t \in (g_{r-1,1}, \dots, g_{r-1,m_{r-1}}, \dots, g_{0,1}, \dots, g_{0,m_0})$ Hence

$$f_t \in (g_1, \dots g_m g_{r-1,1}, \dots g_{r-1,m_{r-1}}, \dots, g_{0,1}, \dots, g_{0,m_0})$$

and so the polynomials $g_1, ..., g_{0,m_0}$ generate a

One of the great successes of category theory in computer science has been the development of a "unified theory" of the constructions underlying denotational semantics. In the untyped λ -calculus, any term may appear in the function position of an application. This means that a model D of the λ -calculus must have the property that given a term t whose interpretation is $d \in D$, Also, the interpretation of a functional abstraction like $\lambda x \cdot x$ is most conveniently defined as a function from DtoD, which must then be regarded element of D. as an Let $\psi: [D \to D] \to D$ be the function that picks out elements of D to represent elements of $[D \rightarrow D]$ and $\phi: D \rightarrow [D \rightarrow D]$ be the function that maps elements of D to functions of D. Since $\psi(f)$ is intended to represent the function f as an element of D, it makes sense to require that $\phi(\psi(f)) = f$, that is, $\psi o \psi = id_{[D \to D]}$ Furthermore, we often want to view every element of D as representing some function from D to D and require that elements representing the same function be equal - that is $\psi(\varphi(d)) = d$

or

 $\psi o \phi = id_D$

The latter condition is called extensionality. These conditions together imply that ϕ and ψ are inverses--- that is, D is isomorphic to the space of functions from D to D that can be the interpretations of functional abstractions: $D \cong [D \rightarrow D]$. Let us suppose we are working with the untyped λ -calculus, we need a solution of the equation $D \cong A + [D \rightarrow D],$ where Α is some predetermined domain containing interpretations for elements of C. Each element of D corresponds to either an element of A or an element of $[D \rightarrow D]$, with a tag. This equation can be solved by finding least fixed points of the function $F(X) = A + [X \rightarrow X]$ from domains to domains --- that is, finding domains X such that



 $X \cong A + [X \longrightarrow X]$, and such that for any domain *Y* also satisfying this equation, there is an embedding of *X* to *Y* --- a pair of maps

$$X \square_{f^R}$$

Such that $f^R \circ f = id_X$ $f \circ f^R \subset id_Y$

Where $f \subseteq g$ means

that

f approximates g in some ordering representing their information content. The key shift of perspective from the domain-theoretic to the more general category-theoretic approach lies in considering F not as a function on domains, but as a *functor* on a category of domains. Instead of a least fixed point of the function, F.

Definition 1.3: Let K be a category and $F: K \to K$ as a functor. A fixed point of F is a pair (A,a), where A is a **K-object** and $a: F(A) \to A$ is an isomorphism. A prefixed point of F is a pair (A,a), where A is a **K-object** and a is any arrow from F(A) to A

Definition 1.4: An ω -chain in a category **K** is a diagram of the following form:

$$\Delta = D_o \xrightarrow{f_o} D_1 \xrightarrow{f_1} D_2 \xrightarrow{f_2} \cdots$$

Recall that a cocone μ of an ω -chain Δ is a K-object X and a collection of K $\{\mu_i: D_i \to X \mid i \ge 0\}$ -arrows such that $\mu_i = \mu_{i+1} o f_i$ for all $i \ge 0$. We sometimes write $\mu: \Delta \to X$ as a reminder of the arrangement of μ 's components Similarly, a colimit $\mu: \Delta \to X$ is a cocone with the property that if $\nu: \Delta \to X'$ is also a cocone then there exists a unique mediating $k: X \to X'$ arrow such that for all $i \ge 0, v_i = k o \mu_i$. Colimits of ω -chains are sometimes referred to as $\omega - co \lim its$. Dually, an ω^{op} - chain in **K** is a diagram of the following form:

 $\Delta = D_o \underbrace{\stackrel{f_o}{\longleftarrow} D_1} \underbrace{\stackrel{f_1}{\longleftarrow} D_2} \underbrace{\stackrel{f_2}{\longleftarrow} \cdots \cdots}_{H}$

 $\mu: X \to \Delta \text{ of an } \omega^{op} - chain \Delta \text{ is a } \mathbf{K}\text{-object X}$ and a collection of **K**-arrows $\{\mu_i: D_i \mid i \ge 0\}$ such that for all $i \ge 0$, $\mu_i = f_i \circ \mu_{i+1}$. An ω^{op} -limit of an $\omega^{op} - chain \Delta$ is a cone $\mu: X \to \Delta$ with the property that if $\nu: X' \to \Delta$ is also a cone, then there exists a unique mediating arrow $k: X' \to X$ such that for all $i \ge 0, \mu_i \ o \ k = \nu_i$. We write \bot_k (or just \bot) for the distinguish initial object of K, when it has one, and $\bot \to A$ for the unique arrow from \bot to each K-object A. It is also convenient to write $\Delta^- = D_1 \xrightarrow{f_1} D_2 \xrightarrow{f_2} \dots$ to denote all of Δ except D_o and f_0 . By analogy, μ^- is $\{\mu_i \mid i \ge 1\}$. For the images of Δ and μ under F we write $F(\Delta) = F(D_o) \xrightarrow{F(f_o)} F(D_1) \xrightarrow{F(f_1)} F(D_2) \xrightarrow{F(f_2)} \dots$ and $F(\mu) = \{F(\mu_i) \mid i \ge 0\}$

We write F^i for the *i*-fold iterated composition of F— that is, $F^o(f) = f, F^1(f) = F(f), F^2(f) = F(F(f))$,etc. With these definitions we can state that every monitonic function on a complete lattice has a least fixed point:

Lemma 1.4. Let *K* be a category with initial object \bot and let $F: K \to K$ be a functor. Define the $\omega - chain \Delta$ by

 $\Delta = \bot \xrightarrow{\mu \to F(\bot)} F(\bot) \xrightarrow{F(\amalg \to F(\bot))} F^2(\amalg \to F(\bot))$ If both $\mu : \Delta \to D$ and $F(\mu) : F(\Delta) \to F(D)$ are colimits, then (D,d) is an initial F-algebra, where $d : F(D) \to D$ is the mediating arrow from $F(\mu)$ to the cocone μ^-

Theorem 1.4 Let a DAG G given in which each node is a random variable, and let a discrete conditional probability distribution of each node given values of its parents in G be specified. Then the product of these conditional distributions yields a joint probability distribution P of the variables, and (G,P) satisfies the Markov condition.

Proof. Order the nodes according to an ancestral ordering. Let X_1, X_2, \dots, X_n be the resultant ordering. Next define.

$$P(x_1, x_2, \dots, x_n) = P(x_n | pa_n) P(x_{n-1} | Pa_{n-1}) \dots$$

...P(x_2 | pa_2)P(x_1 | pa_1),

Where PA_i is the set of parents of X_i of in G and $P(x_i | pa_i)$ is the specified conditional probability distribution. First we show this does

cone



indeed yield a joint probability distribution. Clearly, $0 \le P(x_1, x_2, ..., x_n) \le 1$ for all values of the variables. Therefore, to show we have a joint distribution, as the variables range through all their possible values, is equal to one. To that end, Specified conditional distributions are the conditional distributions they notationally represent in the joint distribution. Finally, we show the Markov condition is satisfied. To do this, we need show for $1 \le k \le n$ that whenever

$$P(pa_k) \neq 0, if \ P(nd_k \mid pa_k) \neq 0$$

and
$$P(x_k \mid pa_k) \neq 0$$

then $P(x_k \mid nd_k, pa_k) = P(x_k \mid pa_k)$,

Where ND_k is the set of nondescendents of X_k of in G. Since $PA_k \subseteq ND_k$, we need only show $P(x_k \mid nd_k) = P(x_k \mid pa_k)$. First for a given k, order the nodes so that all and only nondescendents of X_k precede X_k in the ordering. Note that this ordering depends on k, whereas the ordering in the first part of the proof does not. Clearly then

$$ND_{k} = \{X_{1}, X_{2}, \dots, X_{k-1}\}$$

Let
$$D_{k} = \{X_{k+1}, X_{k+2}, \dots, X_{n}\}$$

 Σ

follows \sum_{d_1}

We define the m^{th} cyclotomic field to be the field $Q[x]/(\Phi_m(x))$ Where $\Phi_m(x)$ is the m^{th} cyclotomic polynomial. $Q[x]/(\Phi_m(x))$ $\Phi_m(x)$ has degree $\varphi(m)$ over Q since $\Phi_m(x)$ has degree $\varphi(m)$. The roots of $\Phi_m(x)$ are just the primitive m^{th} roots of unity, so the complex embeddings of $Q[x]/(\Phi_m(x))$ are simply the $\varphi(m)$ maps

$$\sigma_{k}: Q[x]/(\Phi_{m}(x)) \mapsto C,$$

$$1 \leq k \prec m, (k,m) = 1, \quad where$$

$$\sigma_{k}(x) = \xi_{m}^{k},$$

 ξ_m being our fixed choice of primitive m^{th} root of unity. Note that $\xi_m^k \in Q(\xi_m)$ for every k; it follows that $Q(\xi_m) = Q(\xi_m^k)$ for all k relatively prime to m. In particular, the images of the σ_i coincide, so $Q[x]/(\Phi_m(x))$ is Galois over Q. This means that

we can write $Q(\xi_m)$ for $Q[x]/(\Phi_m(x))$ without much fear of ambiguity; we will do so from now on, the identification being $\xi_m \mapsto x$. One advantage of this is that one can easily talk about cyclotomic fields being extensions of one another, or intersections or compositums; all of these things take place considering them as subfield of C. We now investigate some basic properties of cyclotomic fields. The first issue is whether or not they are all distinct; to determine this, we need to know which roots of unity lie in $Q(\xi_m)$. Note, for example, that if m is odd, then $-\xi_m$ is a $2m^{th}$ root of unity. We will show that this is the only way in which one can obtain any non- m^{th} roots of unity.

LEMMA 1.5 If *m* divides *n*, then $Q(\xi_m)$ is contained in $Q(\xi_n)$ PROOF. Since $\xi^{n/m} = \xi_m$, we have $\xi_m \in Q(\xi_n)$, so the result is clear

LEMMA 1.6 If m and *n* are relatively prime, then $Q(\xi_m, \xi_n) = Q(\xi_{mm})$

and

 $Q(\xi_m) \cap Q(\xi_n) = Q$

(Recall the $Q(\xi_m, \xi_n)$ is the compositum of $Q(\xi_m)$ and $Q(\xi_n)$)

PROOF. One checks easily that $\xi_m \xi_n$ is a primitive mn^{th} root of unity, so that

$$Q(\xi_{mn}) \subseteq Q(\xi_m, \xi_n)$$

$$[Q(\xi_m, \xi_n): Q] \leq [Q(\xi_m): Q][Q(\xi_n: Q]]$$

$$= \varphi(m)\varphi(n) = \varphi(mn);$$
Since $[Q(\xi_{mn}): Q] = \varphi(mn);$ this implies that $Q(\xi_m, \xi_n) = Q(\xi_{nm})$ We know that $Q(\xi_m, \xi_n)$ has degree $\varphi(mn)$ over Q , so we must have $[Q(\xi_m, \xi_n): Q(\xi_m)] = \varphi(n)$
and $[Q(\xi_m, \xi_n): Q(\xi_m)] = \varphi(m)$

$$[Q(\xi_m): Q(\xi_m) \cap Q(\xi_n)] \geq \varphi(m)$$
And thus that $Q(\xi_m) \cap Q(\xi_n) = Q$
PROPOSITION 1.2 For any m and n



$$Q(\xi_m, \xi_n) = Q(\xi_{[m,n]})$$

And
$$Q(\xi_m) \cap Q(\xi_n) = Q(\xi_{(m,n)});$$

here [m,n] and (m,n) denote the least common multiple and the greatest common divisor of m and n, respectively.

PROOF. Write $m = p_1^{e_1} \dots p_k^{e_k}$ and $p_1^{f_1} \dots p_k^{f_k}$ where the p_i are distinct primes. (We allow $e_i \text{ or } f_i$ to be zero) $Q(\xi_m) = Q(\xi_{p_1^{e_1}})Q(\xi_{p_2^{e_2}})\dots Q(\xi_{p_k^{e_k}})$ and $Q(\xi_n) = Q(\xi_{p_1^{f_1}})Q(\xi_{p_2^{f_2}})\dots Q(\xi_{p_k^{f_k}})$ Thus $Q(\xi_m, \xi_n) = Q(\xi_{p_1^{e_1}})\dots Q(\xi_{p_2^{e_k}})Q(\xi_{p_1^{f_1}})\dots Q(\xi_{p_k^{f_k}})$ $= Q(\xi_{p_1^{e_1}})Q(\xi_{p_1^{f_1}})\dots Q(\xi_{p_k^{e_k}})Q(\xi_{p_k^{f_k}})$ $= Q(\xi_{p_1^{\max(e_{1,f_1})}})\dots Q(\xi_{p_1^{\max(e_{k,f_k})}})$ $= Q(\xi_{p_1^{\max(e_{1,f_1})}})$

An entirely similar computation shows that $Q(\xi_m) \cap Q(\xi_n) = Q(\xi_{(m,n)})$

Mutual information measures the information transferred when x_i is sent and y_i is received, and is defined as

$$I(x_i, y_i) = \log_2 \frac{P(\frac{x_i}{y_i})}{P(x_i)} bits \qquad (1)$$

In a noise-free channel, **each** y_i is uniquely connected to the corresponding x_i , and so they constitute an input –output pair (x_i, y_i) for which

$$P(\overset{x_i}{y_j}) = 1 \text{ and } I(x_i, y_j) = \log_2 \frac{1}{P(x_i)}$$
 bits;

that is, the transferred information is equal to the self-information that corresponds to the input x_i In a very noisy channel, the output y_i and input x_i would be completely uncorrelated, and so $P(\frac{x_i}{y_j}) = P(x_i)$ and also $I(x_i, y_j) = 0$; that is,

there is no transference of information. In general, a given channel will operate between these two extremes. The mutual information is defined between the input and the output of a given channel. An average of the calculation of the mutual information for all input-output pairs of a given channel is the average mutual information:

$$I(X,Y) = \sum_{i,j} P(x_i, y_j) I(x_i, y_j) = \sum_{i,j} P(x_i, y_j) \log_2 \left| \frac{P(x_i/y_j)}{P(x_i)} \right|$$

bits per symbol. This calculation is done over the input and output alphabets. The average mutual information. The following expressions are useful for modifying the mutual information expression:

$$P(x_{i}, y_{j}) = P(\overset{x_{i}}{/y_{j}})P(y_{j}) = P(\overset{y_{j}}{/x_{i}})P(x_{i})$$

$$P(y_{j}) = \sum_{i} P(\overset{y_{j}}{/x_{i}})P(x_{i})$$

$$P(x_{i}) = \sum_{i} P(\overset{x_{i}}{/y_{j}})P(y_{j})$$
Then
$$I(X, Y) = \sum_{i,j} P(x_{i}, y_{j}) \log_{2}\left[\frac{1}{P(x_{i})}\right]$$

$$-\sum_{i,j} P(x_{i}, y_{j}) \log_{2}\left[\frac{1}{P(\overset{x_{i}}{/y_{j}})}\right]$$

$$\sum_{i,j} P(x_{i}, y_{j}) \log_{2}\left[\frac{1}{P(x_{i})}\right]$$

$$= \sum_{i} \left[P(\overset{x_{i}}{/y_{j}})P(y_{j}) \right] \log_{2}\frac{1}{P(x_{i})}$$

$$\sum_{i} P(x_{i}) \log_{2}\frac{1}{P(x_{i})} = H(X)$$

$$I(X, Y) = H(X) - H(\overset{X}{/Y})$$
Where $H(\overset{X}{/Y}) = \sum_{i,j} P(x_{i}, y_{j}) \log_{2}\frac{1}{P(\overset{x_{i}}{/y_{j}})}$

is usually called the equivocation. In a sense, the equivocation can be seen as the information lost in the noisy channel, and is a function of the backward conditional probability. The observation of an output symbol y_j provides H(X) - H(X/Y) bits of information. This difference is the mutual



information of the channel. *Mutual Information: Properties* Since

$$P(\frac{x_i}{y_j})P(y_j) = P(\frac{y_j}{x_i})P(x_i)$$

The mutual information fits the condition

I(X,Y) = I(Y,X)

And by interchanging input and output it is also true that

$$I(X,Y) = H(Y) - H(\frac{Y}{X})$$

Where

$$H(Y) = \sum_{j} P(y_{j}) \log_{2} \frac{1}{P(y_{j})}$$

This last entropy is usually called the noise entropy. Thus, the information transferred through the channel is the difference between the output entropy and the noise entropy. Alternatively, it can be said that the channel mutual information is the difference between the number of bits needed for determining a given input symbol before knowing the corresponding output symbol, and the number of bits needed for determining a given input symbol after knowing the corresponding output symbol

$$I(X,Y) = H(X) - H(X/Y)$$

As the channel mutual information expression is a difference between two quantities, it seems that this parameter can adopt negative values. However, and is spite of the fact that for some y_j , $H(X / y_j)$ can be larger than H(X), this is not possible for the average value calculated over all the outputs:

$$\sum_{i,j} P(x_i, y_j) \log_2 \frac{\frac{P(x_i/y_j)}{y_j}}{P(x_i)} = \sum_{i,j} P(x_i, y_j) \log_2 \frac{P(x_i, y_j)}{P(x_i)P(y_j)}$$

Then

$$-I(X,Y) = \sum_{i,j} P(x_i, y_j) \frac{P(x_i)P(y_j)}{P(x_i, y_j)} \le 0$$

Because this expression is of the form

$$\sum_{i=1}^{M} P_i \log_2(\frac{Q_i}{P_i}) \le 0$$

The above expression can be applied due to the factor $P(x_i)P(y_j)$, which is the product of two probabilities, so that it behaves as the quantity Q_i , which in this expression is a dummy variable that fits the condition $\sum_i Q_i \leq 1$. It can be concluded that the average mutual information is a nonnegative number. It can also be equal to zero, when the input and the output are independent of each other. A related entropy called the joint entropy is defined as

$$H(X,Y) = \sum_{i,j} P(x_i, y_j) \log_2 \frac{1}{P(x_i, y_j)}$$
$$= \sum_{i,j} P(x_i, y_j) \log_2 \frac{P(x_i)P(y_j)}{P(x_i, y_j)}$$
$$+ \sum_{i,j} P(x_i, y_j) \log_2 \frac{1}{P(x_i)P(y_j)}$$

Theorem 1.5: Entropies of the binary erasure channel (BEC) The BEC is defined with an alphabet of two inputs and three outputs, with symbol probabilities.

 $P(x_1) = \alpha$ and $P(x_2) = 1 - \alpha$, and transition probabilities

$$P(\frac{y_3}{x_2}) = 1 - p \text{ and } P(\frac{y_2}{x_1}) = 0,$$

and $P(\frac{y_3}{x_1}) = 0$
and $P(\frac{y_1}{x_2}) = p$
and $P(\frac{y_1}{x_2}) = 1 - p$

Lemma 1.7. Given an arbitrary restricted timediscrete, amplitude-continuous channel whose restrictions are determined by sets F_n and whose density functions exhibit no dependence on the state s, let n be a fixed positive integer, and p(x) an arbitrary probability density function on Euclidean n-space. p(y|x) for the density $p_n(y_1,...,y_n | x_1,...x_n)$ and F for F_n . For any real number a, let

$$A = \left\{ (x, y) : \log \frac{p(y \mid x)}{p(y)} > a \right\}$$
(1)

Then for each positive integer u, there is a code (u, n, λ) such that

$$\lambda \le ue^{-a} + P\{(X,Y) \notin A\} + P\{X \notin F\}$$
(2)

Where

 $P\{(X,Y) \in A\} = \int_A \dots \int p(x,y) dx dy, \qquad p(x,y) = p(x)p(y \mid x)$ and

$$P\left\{X \in F\right\} = \int_F \dots \int p(x) dx$$

Proof: A sequence $x^{(1)} \in F$ such that $P\left\{Y \in A_{x^1} \mid X = x^{(1)}\right\} \ge 1 - \varepsilon$ where $A_x = \left\{y : (x, y) \in A\right\};$

Choose the decoding set B_1 to be $A_{x^{(1)}}$. Having chosen $x^{(1)}, \ldots, x^{(k-1)}$ and B_1, \ldots, B_{k-1} , select $x^k \in F$ such that



$$P\left\{Y \in A_{x^{(k)}} - \bigcup_{i=1}^{k-1} B_i \mid X = x^{(k)}\right\} \ge 1 - \varepsilon;$$

Set $B_k = A_{x^{(k)}} - \bigcup_{i=1}^{k-1} B_i$, If the process does not terminate in a finite number of steps, then the sequences $x^{(i)}$ and decoding sets B_i , i = 1, 2, ..., u, form the desired code. Thus assume that the process terminates after t steps. (Conceivably t = 0). We will show $t \ge u$ by showing that $\varepsilon \le te^{-a} + P\{(X, Y) \notin A\} + P\{X \notin F\}$. We proceed as follows.

Let

$$B = \bigcup_{j=1}^{t} B_{j}. \quad (If \ t = 0, \ take \ B = \phi). \ Then$$
$$P\{(X, Y) \in A\} = \int_{(x, y) \in A} p(x, y) dx dy$$
$$= \int_{x} p(x) \int_{y \in A_{x}} p(y \mid x) dy dx$$
$$= \int p(x) \int p(y \mid x) dy dx + \int p(x)$$

F.Algorithms

x

Ideals. Let A be a ring. Recall that an *ideal a* in A is a subset such that a is subgroup of A regarded as a group under addition;

x

 $a \in a, r \in A \Longrightarrow ra \in A$

 $y \in B \cap A$

The ideal generated by a subset S of A is the intersection of all ideals A containing a ----- it is easy to verify that this is in fact an ideal, and that it consist of all finite sums of the form $\sum r_i s_i$ with $r_i \in A, s_i \in S$. When $S = \{s_1, \ldots, s_m\}$, we shall write (s_1, \ldots, s_m) for the ideal it generates. Let a and b be ideals in A. The set

 $\{a+b \mid a \in a, b \in b\}$ is an ideal, denoted by a+b. The ideal generated by $\{ab \mid a \in a, b \in b\}$ is denoted by ab. Note that $ab \subset a \cap b$. Clearly ab consists of all finite sums $\sum a_i b_i$ with $a_i \in a$ and $b_i \in b$, and if $a = (a_1, ..., a_m)$ and $b = (b_1, ..., b_n)$, then $ab = (a_1b_1, ..., a_ib_j, ..., a_mb_n)$. Let a be an ideal of A. The set of cosets of a in A forms a ring A/a, and $a \mapsto a+a$ is a homomorphism $\phi: A \mapsto A/a$. The map $b \mapsto \phi^{-1}(b)$ is a one to one correspondence between the ideals of A/a and the ideals of A containing a An ideal p if prime if

 $p \neq A$ and $ab \in p \Longrightarrow a \in p$ or $b \in p$. Thus p is prime if and only if A / p is nonzero and has the property that ab = 0, $b \neq 0 \Longrightarrow a = 0$, i.e., A/p is an integral domain. An ideal *m* is *maximal* if $m \neq A$ and there does not exist an ideal n contained strictly between m and A. Thus m is maximal if and only if A/m has no proper nonzero ideals, and so is a field. Note that m maximal \Rightarrow *m* prime. The ideals of $A \times B$ are all of the form $a \times b$, with a and b ideals in A and B. To see this, note that if c is an ideal in $A \times B$ and $(a,b) \in c$, then $(a,0) = (a,b)(1,0) \in c$ and $(0,b) = (a,b)(0,1) \in c$. This shows that $c = a \times b$ with

 $a = \{a \mid (a,b) \in c \text{ some } b \in b\}$ and $b = \{b \mid (a,b) \in c \text{ some } a \in a\}$

Let A be a ring. An A-algebra is a ring B together with a homomorphism $i_B : A \to B$. A homomorphism of A -algebra $B \rightarrow C$ is a homomorphism of rings $\varphi: B \to C$ such that $\varphi(i_B(a)) = i_C(a)$ for all $a \in A$. An A-algebra B is said to be *finitely generated* (or of *finite-type* over A) if there exist elements $x_1, ..., x_n \in B$ such that every element of B can be expressed as a polynomial in the x_i with coefficients in i(A), i.e., such that the homomorphism $A[X_1,...,X_n] \rightarrow B$ sending X_i to x_i is surjective. A ring homomorphism $A \rightarrow B$ is *finite*, and B is finitely generated as an A-module. Let k be a field, and let A be a k -algebra. If $1 \neq 0$ in A, then the map $k \rightarrow A$ is injective, we can identify k with its image, i.e., we can regard k as a subring of A. If 1=0 in a ring R, the R is the zero ring, i.e., $R = \{0\}$. **Polynomial rings.** Let k be a field. A monomial in $X_1, ..., X_n$ is an expression of the form $X_1^{a_1}...X_n^{a_n}, \qquad a_j \in N$. The total degree of the monomial is $\sum a_i$. We sometimes abbreviate it by $X^{\alpha}, \alpha = (a_1, ..., a_n) \in \square^n$ The elements of the polynomial ring $k[X_1,...,X_n]$ are finite sums $\sum c_{a_1\dots a_n} X_1^{a_1} \dots X_n^{a_n}, \qquad c_{a_1\dots a_n} \in k, \quad a_j \in \square$



With the obvious notions of equality, addition and multiplication. Thus the monomials from basis for $k[X_1,...,X_n]$ as a k -vector space. The ring $k[X_1,...,X_n]$ is an integral domain, and the only units in it are the nonzero constant polynomials. A polynomial $f(X_1,...,X_n)$ is *irreducible* if it is nonconstant and has only the obvious factorizations, i.e., $f = gh \Longrightarrow g$ or h is constant. Division in k[X]. The division algorithm allows us to divide a nonzero polynomial into another: let f and g be polynomials in k[X] with $g \neq 0$; then there exist unique polynomials $q, r \in k[X]$ such that f = qg + r with either r = 0 or deg $r < \deg g$. Moreover, there is an algorithm for deciding whether $f \in (g)$, namely, find r and check whether it is zero. Moreover, the Euclidean algorithm allows to pass from finite set of generators for an ideal in k X to a single generator by successively replacing each pair of generators with their greatest common divisor.

(*Pure*) **lexicographic** ordering (lex). Here monomials are ordered by lexicographic(dictionary) order. More precisely, let $\alpha = (a_1, ..., a_n)$ and $\beta = (b_1, ..., b_n)$ be two elements of \Box^n ; then $\alpha > \beta$ and $X^{\alpha} > X^{\beta}$ (lexicographic ordering) if, in the vector difference $\alpha - \beta \in \Box$, the left most nonzero entry is positive. For example,

 $XY^2 > Y^3Z^4$; $X^3Y^2Z^4 > X^3Y^2Z$. Note that this isn't quite how the dictionary would order them: it would put *XXXYYZZZZ* after *XXXYYZ*. *Graded reverse lexicographic order (grevlex)*. Here monomials are ordered by total degree, with ties broken by reverse lexicographic ordering. Thus, $\alpha > \beta$ if $\sum a_i > \sum b_i$, or $\sum a_i = \sum b_i$ and in $\alpha - \beta$ the right most nonzero entry is negative. For example:

$$X^{4}Y^{4}Z^{7} > X^{5}Y^{5}Z^{4} \text{ (total degree greater)}$$
$$XY^{5}Z^{2} > X^{4}YZ^{3}, \quad X^{5}YZ > X^{4}YZ^{2}$$

Orderings on $k[X_1,...X_n]$. Fix an ordering on the monomials in $k[X_1,...X_n]$. Then we can write an element f of $k[X_1,...X_n]$ in a canonical fashion, by re-ordering its elements in decreasing order. For example, we would write

$$f = 4XY^{2}Z + 4Z^{2} - 5X^{3} + 7X^{2}Z^{2}$$
as
$$f = -5X^{3} + 7X^{2}Z^{2} + 4XY^{2}Z + 4Z^{2} \quad (lex)$$
or
$$f = 4XY^{2}Z + 7X^{2}Z^{2} - 5X^{3} + 4Z^{2} \quad (grevlex)$$
Let
$$\sum a X^{\alpha} \in k[X, ..., X]$$
in decreasing

Let $\sum \alpha_{\alpha} X \in \mathcal{K}[X_1, ..., X_n]$, in decreasing order: $f = \alpha_{\alpha_0} X^{\alpha_0} +_{\alpha_1} X^{\alpha_1} + ..., \qquad \alpha_0 > \alpha_1 > ..., \quad \alpha_0 \neq 0$

Then we define.

- The multidegree of f to be multdeg(f) = α_0 ;
- The leading coefficient of f to be $LC(f) = a_{\alpha_0}$;
- The leading monomial of f to be $LM(f) = X^{\alpha_0}$;
- The leading term of f to be $LT(f) = a_{\alpha_0} X^{\alpha_0}$

For the polynomial $f = 4XY^2Z + \dots$, the multidegree is (1,2,1), the leading coefficient is 4, the leading monomial is XY^2Z , and the leading term is $4XY^2Z$. The division algorithm in $k[X_1,...X_n]$. Fix a monomial ordering in \square^2 . Suppose given a polynomial f and an ordered set (g_1, \dots, g_s) of polynomials; the division algorithm then constructs polynomials a_1, \dots, a_s and r such that $f = a_1 g_1 + ... + a_s g_s + r$ Where either r = 0 or no monomial in r is divisible by any of $LT(g_1), \dots, LT(g_s)$ Step 1: If $LT(g_1)|LT(f)$, divide g_1 into f to get $f = a_1g_1 + h, \qquad a_1 = \frac{LT(f)}{LT(g_1)} \in k[X_1, ..., X_n]$ If $LT(g_1) | LT(h)$, repeat the process until $f = a_1g_1 + f_1$ (different a_1) with $LT(f_1)$ not divisible by $LT(g_1)$. Now divide g_2 into f_1 , and so on, until $f = a_1g_1 + ... + a_sg_s + r_1$ With $LT(r_1)$ not divisible by any $LT(g_1), ..., LT(g_s)$ **Step 2:** Rewrite $r_1 = LT(r_1) + r_2$, and repeat Step 1 f with r_2 for : $f = a_1g_1 + \dots + a_sg_s + LT(r_1) + r_3$ (different a_i 's) Monomial ideals. In general, an ideal awill contain a polynomial without containing the individual terms of the polynomial; for example, the

International Journal Of Computational Engineering Research (ijceronline.com) Vol. 2 Issue. 7

ideal $a = (Y^2 - X^3)$ contains $Y^2 - X^3$ but not Y^2 or X^3 .

DEFINITION 1.5. An ideal *a* is monomial if $\sum c_{\alpha} X^{\alpha} \in a \Longrightarrow X^{\alpha} \in a$

all α with $c_{\alpha} \neq 0$.

1 IJCER

PROPOSITION 1.3. Let *a* be a *monomial ideal*, and let $A = \{ \alpha \mid X^{\alpha} \in a \}$. Then *A* satisfies the condition $\alpha \in A$, $\beta \in \square^n \Rightarrow \alpha + \beta \in$ (*) And *a* is the *k*-subspace of $k[X_1,...,X_n]$ generated by the $X^{\alpha}, \alpha \in A$. Conversely, of *A* is a subset of \square^n satisfying (*), then the k-subspace *a* of $k[X_1,...,X_n]$ generated by $\{X^{\alpha} \mid \alpha \in A\}$ is a monomial ideal.

PROOF. It is clear from its definition that a monomial ideal a is the k-subspace of $k[X_1,...,X_n]$ generated by the set of monomials it contains. If

generated by the set of monomials it contains. If $X^{\alpha} \in a_{\text{and}} X^{\beta} \in k[X_1,...,X_n]$.

If a permutation is chosen uniformly and at random from the n! possible permutations in S_n , then the counts $C_j^{(n)}$ of cycles of length j are dependent random variables. The joint distribution of $C^{(n)} = (C_1^{(n)}, ..., C_n^{(n)})$ follows from Cauchy's formula, and is given by

$$P[C^{(n)} = c] = \frac{1}{n!} N(n, c) = 1 \left\{ \sum_{j=1}^{n} jc_j = n \right\} \prod_{j=1}^{n} \left(\frac{1}{j}\right)^{c_j} \frac{1}{c_j!}, \quad (1.1)$$

for $c \in \square_+^n$.

Lemma1.7 For nonnegative integers $m_{1,...}m_n$,

$$E\left(\prod_{j=1}^{n} (C_{j}^{(n)})^{[m_{j}]}\right) = \left(\prod_{j=1}^{n} \left(\frac{1}{j}\right)^{m_{j}}\right) \left\{\sum_{j=1}^{n} jm_{j} \le n\right\}$$
(1.4)

Proof. This can be established directly by exploiting cancellation of the form $c_j^{[m_j]}/c_j^! = 1/(c_j - m_j)!$ when $c_j \ge m_j$, which occurs between the ingredients in Cauchy's formula and the falling factorials in the moments. Write $m = \sum jm_j$. Then, with the first sum indexed by $c = (c_1, ..., c_n) \in \square_+^n$ and the last sum indexed by

 $d = (d_1, ..., d_n) \in \square_+^n \text{ via the correspondence}$ $d_j = c_j - m_j, \text{ we have}$ $E\left(\prod_{j=1}^n (C_j^{(n)})^{[m_j]}\right) = \sum_c P[C^{(n)} = c] \prod_{j=1}^n (c_j)^{[m_j]}$ $= \sum_{cx_j \ge m_j \text{ for all } j} \left\{\sum_{j=1}^n jc_j = n\right\} \prod_{j=1}^n \frac{(c_j)^{[m_j]}}{j^{c_j}c_j!}$ $= \prod_{j=1}^n \frac{1}{j^{m_j}} \sum_d 1\left\{\sum_{j=1}^n jd_j = n - m\right\} \prod_{j=1}^n \frac{1}{j^{d_j}(d_j)!}$

This last sum simplifies to the indicator $1(m \le n)$, corresponding to the fact that if $n-m \ge 0$, then $d_j = 0$ for j > n-m, and a random permutation in S_{n-m} must have some cycle structure $(d_1, ..., d_{n-m})$. The moments of $C_j^{(n)}$ follow immediately as

$$E(C_j^{(n)})^{[r]} = j^{-r} \mathbb{1}\left\{jr \le n\right\}$$
(1.2)
We note for future reference that (1.4) can also

We note for future reference that (1.4) can also be written in the form

$$E\left(\prod_{j=1}^{n} (C_{j}^{(n)})^{[m_{j}]}\right) = E\left(\prod_{j=1}^{n} Z_{j}^{[m_{j}]}\right) \left\{\sum_{j=1}^{n} jm_{j} \le n\right\},$$
(1.3)

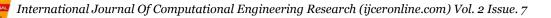
Where the Z_j are independent Poisson-distribution random variables that satisfy $E(Z_j) = 1/j$

The marginal distribution of cycle counts provides a formula for the joint distribution of the cycle counts C_j^n , we find the distribution of C_j^n using a combinatorial approach combined with the inclusion-exclusion formula.

Lemma 1.8. For
$$1 \le j \le n$$
,

$$P[C_{j}^{(n)} = k] = \frac{j^{-k}}{k!} \sum_{l=0}^{\lfloor n/j \rfloor - k} (-1)^{l} \frac{j^{-l}}{l!} \qquad (1.1)$$

Proof. Consider the set I of all possible cycles of length j, formed with elements chosen from $\{1, 2, ..., n\}$, so that $|I| = n^{\lfloor j \lor j \rfloor}$. For each $\alpha \in I$, consider the "property" G_{α} of having α ; that is, G_{α} is the set of permutations $\pi \in S_n$ such that α is one of the cycles of π . We then have $|G_{\alpha}| = (n - j)!$, since the elements of $\{1, 2, ..., n\}$ not in α must be permuted among themselves. To use the inclusion-exclusion formula we need to calculate the term S_r , which is the sum of the probabilities of the r-fold intersection of properties, summing over all sets of r distinct properties. There



are two cases to consider. If the *r* properties are indexed by *r* cycles having no elements in common, then the intersection specifies how *rj* elements are moved by the permutation, and there are $(n-rj)!1(rj \le n)$ permutations in the intersection. There are $n^{[rj]}/(j^r r!)$ such intersections. For the other case, some two distinct properties name some element in common, so no permutation can have both these properties, and the *r*-fold intersection is empty. Thus

$$S_{r} = (n - rj)! l(rj \le n)$$

 $\times \frac{n^{[rj]}}{j^{r}r!} \frac{1}{n!} = l(rj \le n) \frac{1}{j^{r}r!}$

Finally, the inclusion-exclusion series for the number of permutations having exactly k properties is

$$\sum_{l\geq 0} (-1)^l \binom{k+l}{l} S_{k+l,}$$

Which simplifies to (1.1) Returning to the original hat-check problem, we substitute j=1 in (1.1) to obtain the distribution of the number of fixed points of a random permutation. For k = 0, 1, ..., n,

$$P[C_1^{(n)} = k] = \frac{1}{k!} \sum_{l=0}^{n-k} (-1)^l \frac{1}{l!},$$
 (1.2)

and the moments of $C_1^{(n)}$ follow from (1.2) with j = 1. In particular, for $n \ge 2$, the mean and variance of $C_1^{(n)}$ are both equal to 1. The joint distribution of $(C_1^{(n)}, ..., C_b^{(n)})$ for any $1 \le b \le n$ has an expression similar to (1.7); this too can be derived by inclusion-exclusion. For any $c = (c_1, ..., c_b) \in \Box_+^b$ with $m = \sum ic_i$, $P[(C_1^{(n)}, ..., C_b^{(n)}) = c] = \left\{ \prod_{i=1}^b \left(\frac{1}{i}\right)^{c_i} \frac{1}{c_i!} \right\} \sum_{\substack{l \ge 0 \text{ with} \\ \sum l_l \le n = m}} (-1)^{l_1 + ... + l_b} \prod_{i=1}^b \left(\frac{1}{i}\right)^{l_i} \frac{1}{l_i!}$ (1.3)

The joint moments of the first *b* counts $C_1^{(n)}, ..., C_b^{(n)}$ can be obtained directly from (1.2) and (1.3) by setting $m_{b+1} = ... = m_n = 0$

The limit distribution of cycle counts

It follows immediately from Lemma 1.2 that for each fixed j, as $n \to \infty$, $P[C_j^{(n)} = k] \to \frac{j^{-k}}{k!} e^{-1/j}, \quad k = 0, 1, 2, ...,$ So that $C_j^{(n)}$ converges in distribution to a random variable Z_j having a Poisson distribution with mean 1/j; we use the notation $C_j^{(n)} \rightarrow_d Z_j$ where $Z_j \square P_o(1/j)$ to describe this. Infact, the limit random variables are independent.

Theorem 1.6 The process of cycle counts converges in distribution to a Poisson process of \Box

with intensity j^{-1} . That is, as $n \to \infty$,

$$(C_1^{(n)}, C_2^{(n)}, ...) \to_d (Z_1, Z_2, ...)$$
 (1.1)

Where the Z_j , j = 1, 2, ..., are independent Poisson-distributed random variables with

$$E(Z_j) = \frac{1}{j}$$

Proof. To establish the converges in distribution one shows that for each fixed $b \ge 1$, as $n \to \infty$,

$$P[(C_1^{(n)},...,C_b^{(n)})=c] \to P[(Z_1,...,Z_b)=c]$$

Error rates

The proof of Theorem says nothing about the rate of convergence. Elementary analysis can be used to estimate this rate when b=1. Using properties of alternating series with decreasing terms, for k=0,1,...,n,

$$\frac{1}{k!} \left(\frac{1}{(n-k+1)!} - \frac{1}{(n-k+2)!}\right) \le \left| P[C_1^{(n)} = k] - P[Z_1 = k] \right|$$
$$\le \frac{1}{k!(n-k+1)!}$$

It follows that

$$\frac{2^{n+1}}{(n+1)!} \frac{n}{n+2} \le \sum_{k=0}^{n} \left| P[C_1^{(n)} = k] - P[Z_1 = k] \right| \le \frac{2^{n+1} - 1}{(n+1)!} \quad (1.11)$$

Since

$$P[Z_1 > n] = \frac{e^{-1}}{(n+1)!} (1 + \frac{1}{n+2} + \frac{1}{(n+2)(n+3)} + \dots) < \frac{1}{(n+1)!},$$

We see from (1.11) that the total variation distance between the distribution $L(C_1^{(n)})$ of $C_1^{(n)}$ and the distribution $L(Z_1)$ of Z_1

Establish the asymptotics of $P[A_n(C^{(n)})]$ under conditions (A_0) and (B_{01}) , where



$$\begin{split} A_{n}(C^{(n)}) &= \bigcap_{1 \le i \le n} \bigcap_{r_{i}+1 \le j \le r_{i}} \left\{ C_{ij}^{(n)} = 0 \right\}, \\ \text{and } \zeta_{i} &= (r_{i}^{'} / r_{id}) - 1 = O(i^{-g}) \text{ as } i \to \infty, \text{ for some } g^{'} > 0. \text{ We start with the expression} \\ P[A_{n}(C^{(n)})] &= \frac{P[T_{0m}(Z^{'}) = n]}{P[T_{0m}(Z) = n]} \\ \prod_{\substack{1 \le i \le n \\ r_{i}+1 \le j \le r_{i}}} \left\{ 1 - \frac{\theta}{ir_{i}} (1 + E_{i0}) \right\} \quad (1.1) \\ P[T_{0n}(Z^{'}) = n] \\ &= \frac{\theta d}{n} \exp\left\{ \sum_{i \ge 1} [\log(1 + i^{-1}\theta d) - i^{-1}\theta d] \right\} \\ \left\{ 1 + O(n^{-1}\varphi_{\{1,2,7\}}(n)) \right\} \quad (1.2) \\ \text{and} \\ P[T_{0n}(Z^{'}) = n] \\ &= \frac{\theta d}{n} \exp\left\{ \sum_{i \ge 1} [\log(1 + i^{-1}\theta d) - i^{-1}\theta d] \right\} \\ \left\{ 1 + O(n^{-1}\varphi_{\{1,2,7\}}(n)) \right\} \quad (1.3) \end{split}$$

Where $\varphi_{\{1,2,7\}}(n)$ refers to the quantity derived from Z. It thus follows that $P[A_n(C^{(n)})] \square Kn^{-\theta(1-d)}$ for a constant K, depending on Z and the r_i and computable explicitly from (1.1) - (1.3), if Conditions (A_0) and (B_{01}) are satisfied and if $\zeta_i^* = O(i^{-g})$ from some g > 0, since, under these circumstances, both $n^{-1}\varphi_{\{1,2,7\}}(n)$ and $n^{-1}\varphi_{\{1,2,7\}}(n)$ tend to zero as $n \to \infty$. In particular, for polynomials and square free polynomials, the relative error in this asymptotic approximation is of order n^{-1} if g > 1.

For
$$0 \le b \le n/8$$
 and $n \ge n_0$, with n_0
 $d_{TV}(L(C[1,b]), L(Z[1,b]))$
 $\le d_{TV}(L(C[1,b]), L(Z[1,b]))$
 $\le \varepsilon_{\{7,7\}}(n,b),$

Where $\mathcal{E}_{\{7,7\}}(n,b) = O(b/n)$ under Conditions $(A_0), (D_1)$ and (B_{11}) Since, by the Conditioning Relation,

$$L(C[1,b]|T_{0b}(C) = l) = L(Z[1,b]|T_{0b}(Z) = l),$$

It follows by direct calculation that

$$d_{TV}(L(C[1,b]), L(Z[1,b])) = d_{TV}(L(T_{0b}(C)), L(T_{0b}(Z))) = \max_{A} \sum_{r \in A} P[T_{0b}(Z) = r] = n - r] = \left\{ 1 - \frac{P[T_{bn}(Z) = n - r]}{P[T_{0n}(Z) = n]} \right\}$$
(1.4)

Suppressing the argument Z from now on, we thus obtain

$$\begin{split} &d_{TV}(L(C[1,b]), L(Z[1,b])) \\ &= \sum_{r \ge 0} P[T_{0b} = r] \left\{ 1 - \frac{P[T_{bn} = n - r]}{P[T_{0n} = n]} \right\}_{+} \\ &\leq \sum_{r > n/2} P[T_{0b} = r] + \sum_{r=0}^{[n/2]} \frac{P[T_{0b} = r]}{P[T_{0b} = n]} \\ &\times \left\{ \sum_{s=0}^{n} P[T_{0b} = s](P[T_{bn} = n - s] - P[T_{bn} = n - r]) \right\}_{+} \end{split}$$

$$\leq \sum_{r>n/2} P[T_{0b} = r] + \sum_{r=0}^{\lfloor n/2 \rfloor} P[T_{0b} = r]$$

$$\times \sum_{s=0}^{\lfloor n/2 \rfloor} P[T_{0b} = s] \frac{\{P[T_{bn} = n - s] - P[T_{bn} = n - r]\}}{P[T_{0n} = n]}$$

$$+ \sum_{s=0}^{\lfloor n/2 \rfloor} P[T_{0b} = r] \sum_{s=\lfloor n/2 \rfloor+1}^{n} P[T = s] P[T_{bn} = n - s] / P[T_{0n} = n]$$

The first sum is at most $2n^{-1}ET_{0b}$; the third is bound by

$$\begin{aligned} &(\max_{n/2 < s \le n} P[T_{0b} = s]) / P[T_{0n} = n] \\ &\leq \frac{2\varepsilon_{\{10.5(1)\}}(n/2, b)}{n} \frac{3n}{\theta P_{\theta}[0, 1]}, \\ &\frac{3n}{\theta P_{\theta}[0, 1]} 4n^{-2} \phi_{\{10.8\}}^{*}(n) \sum_{r=0}^{[n/2]} P[T_{0b} = r] \sum_{s=0}^{[n/2]} P[T_{0b} = s] \frac{1}{2} |r-s| \\ &\leq \frac{12\phi_{\{10.8\}}^{*}(n)}{\theta P_{\theta}[0, 1]} \frac{ET_{0b}}{n} \end{aligned}$$

Hence we may take

$$\varepsilon_{\{7,7\}}(n,b) = 2n^{-1}ET_{0b}(Z) \left\{ 1 + \frac{6\phi_{\{10,8\}}^*(n)}{\theta P_{\theta}[0,1]} \right\} P$$
$$+ \frac{6}{\theta P_{\theta}[0,1]} \varepsilon_{\{10,5(1)\}}(n/2,b)$$
(1.5)

Issn 2250-3005(online)



Required order under Conditions $(A_0), (D_1)$ and (B_{11}) , if $S(\infty) < \infty$. If not, $\phi_{(10.8)}^*(n)$ can be replaced by $\phi^*_{\{10,11\}}(n)$ in the above, which has the required order, without the restriction on the r_i implied by $S(\infty) < \infty$. Examining the Conditions $(A_0), (D_1)$ and (B_{11}) , it is perhaps surprising to find that (B_{11}) is required instead of just (B_{01}) ; that is, that we should need $\sum_{l>2} l \mathcal{E}_{il} = O(i^{-a_1})$ to hold for some $a_1 > 1$. A first observation is that a similar problem arises with the rate of decay of \mathcal{E}_{i1} as well. For this reason, n_1 is replaced by n_1 . This makes it possible to replace condition (A_1) by the weaker pair of conditions (A_0) and (D_1) in the eventual assumptions needed for $\mathcal{E}_{(7,7)}(n,b)$ to be of order O(b/n); the decay rate requirement of order $i^{-1-\gamma}$ is shifted from \mathcal{E}_{i1} itself to its first difference. This is needed to obtain the right approximation error for the random mappings example. However, since all the classical applications make far more stringent assumptions about the $\mathcal{E}_{i1}, l \geq 2$, than are made in (B_{11}) . The critical point of the proof is seen where the initial estimate the of difference $P[T_{bn}^{(m)} = s] - P[T_{bn}^{(m)} = s+1]$. The factor $\mathcal{E}_{(10,10)}(n)$, which should be small, contains a far tail element from n_1 of the form $\phi_1^{\theta}(n) + u_1^*(n)$, which is only small if $a_1 > 1$, being otherwise of order $O(n^{1-a_1+\delta})$ for any $\delta > 0$, since $a_2 > 1$ is in any case assumed. For $s \ge n/2$, this gives rise to a contribution of order $O(n^{-1-a_1+\delta})$ in the estimate of the difference $P[T_{bn} = s] - P[T_{bn} = s+1]$, which, in the remainder of the proof, is translated into a contribution of order $O(tn^{-1-a_1+\delta})$ for of the differences form $P[T_{bn} = s] - P[T_{bn} = s+1]$, finally leading to a contribution of order $bn^{-a_1+\delta}$ for any $\delta > 0$ in $\mathcal{E}_{(77)}(n,b)$. Some improvement would seem to be the possible, defining function g by $g(w) = \mathbf{1}_{\{w=s\}} - \mathbf{1}_{\{w=s+t\}}$, differences that are of the form $P[T_{bn} = s] - P[T_{bn} = s+t]$ can be directly estimated, at a cost of only a single contribution of the form $\phi_1^{\theta}(n) + u_1^*(n)$. Then, iterating the cycle, in which one estimate of a difference in point probabilities is improved to an estimate of smaller order, a bound of the form $|P[T_{bn} = s] - P[T_{bn} = s+t]| = O(n^{-2}t + n^{-1-a_1+\delta})$ for any $\delta > 0$ could perhaps be attained, leading to a final error estimate in order $O(bn^{-1} + n^{-a_1+\delta})$ for any $\delta > 0$, to replace $\mathcal{E}_{\{7.7\}}(n,b)$. This would be of the ideal order O(b/n) for large enough b, but would still be coarser for small b.

With b and n as in the previous section, we wish to show that

$$\begin{aligned} \left| d_{TV}(L(C[1,b]), L(Z[1,b])) - \frac{1}{2}(n+1)^{-1} \left| 1 - \theta \right| E \left| T_{0b} - ET_{0b} \right| \\ \leq \varepsilon_{\{7,8\}}(n,b), \end{aligned} \right.$$

Where $\varepsilon_{\{7,8\}}(n,b) = O(n^{-1}b[n^{-1}b + n^{-\beta_{12}+\delta}])$ for any $\delta > 0$ under Conditions $(A_0), (D_1)$ and (B_{12}) , with β_{12} . The proof uses sharper estimates. As before, we begin with the formula

$$d_{TV}(L(C[1,b]), L(Z[1,b])) = \sum_{r \ge 0} P[T_{0b} = r] \left\{ 1 - \frac{P[T_{bn} = n - r]}{P[T_{0n} = n]} \right\}_{+}$$

Now we observe that

$$\begin{split} &\left|\sum_{r\geq 0} P[T_{0b}=r] \left\{ 1 - \frac{P[T_{bn}=n-r]}{P[T_{0n}=n]} \right\}_{+} - \sum_{r=0}^{[n/2]} \frac{P[T_{0b}=r]}{P[T_{0n}=n]} \\ &\times \left|\sum_{s=[n/2]+1}^{n} P[T_{0b}=s] (P[T_{bn}=n-s] - P[T_{bn}=n-r]) \right| \\ &\leq 4n^{-2} E T_{0b}^{2} + (\max_{n/2 < s \le n} P[T_{0b}=s]) / P[T_{0n}=n] \\ &+ P[T_{0b} > n/2] \\ &\leq 8n^{-2} E T_{0b}^{2} + \frac{3\varepsilon_{\{10.5(2)\}}(n/2,b)}{\theta P_{\theta}[0,1]}, \end{split}$$
(1.1)

We have



$$\Big| \sum_{r=0}^{[n/2]} \frac{P[T_{0b} = r]}{P[T_{0n} = n]} \\ \times \Big(\left\{ \sum_{s=0}^{[n/2]} P[T_{0b} = s] (P[T_{bn} = n - s] - P[T_{bn} = n - r] \right\}_{+} \\ - \left\{ \sum_{s=0}^{[n/2]} P[T_{0b} = s] \frac{(s - r)(1 - \theta)}{n + 1} P[T_{0n} = n] \right\}_{+} \Big) \Big|$$

$$\leq \frac{1}{n^{2} P[T_{0n} = n]} \sum_{r \geq 0} P[T_{0b} = r] \sum_{s \geq 0} P[T_{0b} = s] |s - r|$$

$$\times \left\{ \varepsilon_{\{10.14\}}(n, b) + 2(r \vee s) |1 - \theta| n^{-1} \left\{ K_{0} \theta + 4\phi_{\{10.8\}}^{*}(n) \right\} \right\}$$

$$\leq \frac{6}{\theta n P_{\theta}[0, 1]} E T_{0b} \varepsilon_{\{10.14\}}(n, b)$$

$$+ 4 |1 - \theta| n^{-2} E T_{0b}^{2} \left\{ K_{0} \theta + 4\phi_{\{10.8\}}^{*}(n) \right\}$$

$$\left(\frac{3}{\theta n P_{\theta}[0, 1]}\right) \right\}, \qquad (1.2)$$

The approximation in (1.2) is further simplified by noting that

$$\sum_{r=0}^{\lfloor n/2 \rfloor} P[T_{0b} = r] \left\{ \sum_{s=0}^{\lfloor n/2 \rfloor} P[T_{0b} = s] \frac{(s-r)(1-\theta)}{n+1} \right\}_{+}$$

$$-\left\{\sum_{s=0} P[T_{0b} = s] \frac{(s-r)(1-\theta)}{n+1}\right\}_{+} |$$

$$\leq \sum_{r=0}^{\lfloor n/2 \rfloor} P[T_{0b} = r] \sum_{s > \lfloor n/2 \rfloor} P[T_{0b} = s] \frac{(s-r)|1-\theta|}{n+1} |$$

$$\leq |1-\theta| n^{-1} E(T_{0b} 1\{T_{0b} > n/2\}) \leq 2|1-\theta| n^{-2} ET_{0b}^{2}, \quad (1.3)$$

and then by observing that

$$\sum_{r>[n/2]} P[T_{0b} = r] \left\{ \sum_{s\geq 0} P[T_{0b} = s] \frac{(s-r)(1-\theta)}{n+1} \right\}$$

$$\leq n^{-1} |1-\theta| (ET_{0b}P[T_{0b} > n/2] + E(T_{0b}1\{T_{0b} > n/2\}))$$

$$\leq 4 |1-\theta| n^{-2} ET_{0b}^{2}$$
(1.4)

Combining the contributions of (1.2) - (1.3), we thus find that

$$\left| \begin{array}{l} d_{TV}(L(C[1,b]), L(Z[1,b])) \\ -(n+1)^{-1} \sum_{r \ge 0} P[T_{0b} = r] \left\{ \sum_{s \ge 0} P[T_{0b} = s](s-r)(1-\theta) \right\}_{+} \\ \leq \varepsilon_{\{7,8\}}(n,b) \\ = \frac{3}{\theta P_{\theta}[0,1]} \left\{ \varepsilon_{\{10.5(2)\}}(n/2,b) + 2n^{-1}ET_{0b}\varepsilon_{\{10.14\}}(n,b) \right\} \\ + 2n^{-2}ET_{0b}^{2} \left\{ 4 + 3\left|1-\theta\right| + \frac{24\left|1-\theta\right|\phi_{\{10.8\}}^{*}(n)}{\theta P_{\theta}[0,1]} \right\}$$
(1.5)

The quantity $\mathcal{E}_{\{7,8\}}(n,b)$ is seen to be of the order claimed under Conditions $(A_0), (D_1)$ and (B_{12}) , provided that $S(\infty) < \infty$; this supplementary condition can be removed if $\phi_{\{10,8\}}^*(n)$ is replaced by $\phi_{\{10,11\}}^*(n)$ in the definition of $\mathcal{E}_{\{7,8\}}(n,b)$, has the required order without the restriction on the r_i implied by assuming that $S(\infty) < \infty$. Finally, a direct calculation now shows that

$$\sum_{r \ge 0} P[T_{0b} = r] \left\{ \sum_{s \ge 0} P[T_{0b} = s](s - r)(1 - \theta) \right\}_{+}$$
$$= \frac{1}{2} |1 - \theta| E |T_{0b} - ET_{0b}|$$

1.0. Consider Example the point $O = (0, ..., 0) \in \square^n$. For an arbitrary vector r, the coordinates of the point x = O + r are equal to the respective coordinates of the vector $r: x = (x^1, ..., x^n)$ and $r = (x^1, ..., x^n)$. The vector r such as in the example is called the position vector or the radius vector of the point x. (Or, in greater detail: r is the radius-vector of x w.r.t an origin O). Points are frequently specified by their radiusvectors. This presupposes the choice of O as the "standard origin". Let us summarize. We have considered \square^n and interpreted its elements in two ways: as points and as vectors. Hence we may say that we leading with the two copies of $\square^n : \square^n =$ {points}, $\square^n = \{\text{vectors}\}$

Operations with vectors: multiplication by a number, addition. Operations with points and vectors: adding a vector to a point (giving a point), subtracting two points (giving a vector). \Box^n treated in this way is called an *n*-dimensional affine space. (An "abstract" affine space is a pair of sets, the set of points and the set of vectors so that the operations as above are defined axiomatically). Notice that



vectors in an affine space are also known as "free vectors". Intuitively, they are not fixed at points and "float freely" in space. From \Box^n considered as an affine space we can precede in two opposite directions: \Box^n as an Euclidean space $\Leftarrow \Box^n$ as an affine space $\Rightarrow \square^n$ as a manifold.Going to the left means introducing some extra structure which will make the geometry richer. Going to the right means forgetting about part of the affine structure; going further in this direction will lead us to the so-called "smooth (or differentiable) manifolds". The theory of differential forms does not require any extra geometry. So our natural direction is to the right. The Euclidean structure, however, is useful for examples and applications. So let us say a few words about it:

Remark 1.0. Euclidean geometry. In \Box^n considered as an affine space we can already do a good deal of geometry. For example, we can consider lines and planes, and quadric surfaces like an ellipsoid. However, we cannot discuss such things as "lengths", "angles" or "areas" and "volumes". To be able to do so, we have to introduce some more definitions, making \Box^n a Euclidean space. Namely, we define the length of a vector $a = (a^1, \dots, a^n)$ to be

$$|a| := \sqrt{(a^1)^2 + \dots + (a^n)^2}$$
 (1)

After that we can also define distances between points as follows:

$$d(A,B) \coloneqq \left| \overrightarrow{AB} \right| \tag{2}$$

One can check that the distance so defined possesses natural properties that we expect: is it always non-negative and equals zero only for coinciding points; the distance from A to B is the same as that from B to A (symmetry); also, for three C, points, А, В and we have $d(A,B) \le d(A,C) + d(C,B)$ (the "triangle inequality"). To define angles, we first introduce the scalar product of two vectors

$$(a,b) \coloneqq a^1 b^1 + \dots + a^n b^n \tag{3}$$

Thus $|a| = \sqrt{(a,a)}$. The scalar product is also denote by dot: a.b = (a,b), and hence is often referred to as the "dot product". Now, for nonzero vectors, we define the angle between them by the equality

$$\cos \alpha \coloneqq \frac{(a,b)}{|a||b|} \tag{4}$$

The angle itself is defined up to an integral multiple of 2π . For this definition to be consistent we have to ensure that the r.h.s. of (4) does not

exceed 1 by the absolute value. This follows from the inequality

$$(a,b)^{2} \le |a|^{2} |b|^{2}$$
 (5)

known as the Cauchy–Bunyakovsky–Schwarz inequality (various combinations of these three names are applied in different books). One of the ways of proving (5) is to consider the scalar square of the linear combination a+tb, where $t \in R$. As $(a+tb, a+tb) \ge 0$ is a quadratic polynomial in twhich is never negative, its discriminant must be less or equal zero. Writing this explicitly yields (5). The triangle inequality for distances also follows from the inequality (5).

Example 1.1. Consider the function $f(x) = x^{i}$ (the i-th coordinate). The linear function dx^{i} (the differential of x^{i}) applied to an arbitrary vector h is simply h^{i} . From these examples follows that we can rewrite df as

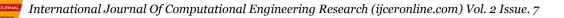
$$df = \frac{\partial f}{\partial x^1} dx^1 + \dots + \frac{\partial f}{\partial x^n} dx^n, \qquad (1)$$

which is the standard form. Once again: the partial derivatives in (1) are just the coefficients (depending on x); dx^1 , dx^2 ,... are linear functions giving on an arbitrary vector h its coordinates h^1 , h^2 ,..., respectively. Hence

$$df(x)(h) = \partial_{hf(x)} = \frac{\partial f}{\partial x^{1}}h^{1} + \dots + \frac{\partial f}{\partial x^{n}}h^{n}, \quad (2)$$

Theorem 1.7. Suppose we have a parametrized curve $t \mapsto x(t)$ passing through $x_0 \in \square^n$ at $t = t_0$ and with the velocity vector $x(t_0) = \upsilon$ Then $\frac{df(x(t))}{dt}(t_0) = \partial_{\upsilon} f(x_0) = df(x_0)(\upsilon)$ (1)

Proof. Indeed, consider a small increment of the parameter $t: t_0 \mapsto t_0 + \Delta t$, Where $\Delta t \mapsto 0$. On the other hand, we have $f(x_0 + h) - f(x_0) = df(x_0)(h) + \beta(h)|h|$ for an arbitrary vector h, where $\beta(h) \to 0$ when $h \to 0$. Combining it together, for the increment of f(x(t)) we obtain



$$f(x(t_0 + \Delta t) - f(x_0))$$

= $df(x_0)(\upsilon.\Delta t + \alpha(\Delta t)\Delta t)$
+ $\beta(\upsilon.\Delta t + \alpha(\Delta t)\Delta t).|\upsilon\Delta t + \alpha(\Delta t)\Delta t|$
= $df(x_0)(\upsilon).\Delta t + \gamma(\Delta t)\Delta t$

For a certain $\gamma(\Delta t)$ such that $\gamma(\Delta t) \rightarrow 0$ when $\Delta t \rightarrow 0$ (we used the linearity of $df(x_0)$). By the definition, this means that the derivative of f(x(t)) at $t = t_0$ is exactly $df(x_0)(v)$. The statement of the theorem can be expressed by a simple formula:

$$\frac{df(x(t))}{dt} = \frac{\partial f}{\partial x^1} x^1 + \dots + \frac{\partial f}{\partial x^n} x^n$$
(2)

To calculate the value Of df at a point x_0 on a given vector v one can take an arbitrary curve passing Through x_0 at t_0 with v as the velocity vector at t_0 and calculate the usual derivative of f(x(t)) at $t = t_0$.

Theorem 1.8. For functions $f, g: U \to \Box$, $U \subset \Box^n$,

$$d(f+g) = df + dg$$
(1)
$$d(fg) = df \cdot g + f \cdot dg$$
(2)

Proof. Consider an arbitrary point x_0 and an arbitrary vector v stretching from it. Let a curve x(t) be such that $x(t_0) = x_0$ and $x(t_0) = v$. Hence

$$d(f+g)(x_0)(\upsilon) = \frac{d}{dt}(f(x(t)) + g(x(t)))$$

at $t = t_0$ and

$$d(fg)(x_0)(v) = \frac{d}{dt}(f(x(t))g(x(t)))$$

at $t = t_0$ Formulae (1) and (2) then immediately follow from the corresponding formulae for the usual derivative Now, almost without change the theory generalizes to functions taking values in \square^m instead of \square . The only difference is that now the differential of a map $F: U \to \square^m$ at a point x will be a linear function taking vectors in \square^n to vectors in \square^m (instead of \square). For an arbitrary vector $h \in |\square^n$,

$$F(x+h) = F(x) + dF(x)(h)$$

+ $\beta(h)|h|$ (3)
Where $\beta(h) \to 0$ when $h \to 0$. We have
 $dF = (dF^1, ..., dF^m)$ and
 $dF = \frac{\partial F}{\partial x^1} dx^1 + ... + \frac{\partial F}{\partial x^n} dx^n$
$$= \begin{pmatrix} \frac{\partial F^1}{\partial x^1} \cdots \frac{\partial F^1}{\partial x^n} \\ \cdots \\ \frac{\partial F^m}{\partial x^1} \cdots \frac{\partial F^m}{\partial x^n} \end{pmatrix} \begin{pmatrix} dx^1 \\ \cdots \\ dx^n \end{pmatrix}$$
 (4)

In this matrix notation we have to write vectors as vector-columns.

Theorem 1.9. For an arbitrary parametrized curve x(t) in \square^n , the differential of a map $F: U \to \square^m$ (where $U \subset \square^n$) maps the velocity vector x(t) to the velocity vector of the curve F(x(t)) in \square^m :

$$\frac{dF(x(t))}{dt} = dF(x(t))(x(t)) \tag{1}$$

Proof. By the definition of the velocity vector,

$$x(t + \Delta t) = x(t) + x(t) \cdot \Delta t + \alpha(\Delta t) \Delta t$$
(2)

Where $\alpha(\Delta t) \rightarrow 0$ when $\Delta t \rightarrow 0$. By the definition of the differential,

$$F(x+h) = F(x) + dF(x)(h) + \beta(h) \left| h \right|$$
(3)

Where $\beta(h) \rightarrow 0$ when $h \rightarrow 0$. we obtain

$$F(x(t + \Delta t)) = F(x + \underbrace{x(t).\Delta t + \alpha(\Delta t)\Delta t}_{h})$$

= $F(x) + dF(x)(x(t)\Delta t + \alpha(\Delta t)\Delta t) +$
 $\beta(x(t)\Delta t + \alpha(\Delta t)\Delta t). \left| x(t)\Delta t + \alpha(\Delta t)\Delta t \right|$
= $F(x) + dF(x)(x(t)\Delta t + \gamma(\Delta t)\Delta t)$

For some $\gamma(\Delta t) \to 0$ when $\Delta t \to 0$. This precisely means that dF(x)x(t) is the velocity vector of F(x). As every vector attached to a point can be viewed as the velocity vector of some curve passing through this point, this theorem gives a clear geometric picture of dF as a linear map on vectors.

🕼 IJCER

Theorem 1.10 Suppose we have two maps $F: U \to V$ and $G: V \to W$, where $U \subset \square^n, V \subset \square^m, W \subset \square^p$ (open domains). Let $F: x \mapsto y = F(x)$. Then the differential of the composite map $GoF: U \to W$ is the composition of the differentials of F and G:d(GoF)(x) = dG(y)odF(x) (4)

Proof. We can use the description of the differential .Consider a curve x(t) in \Box^n with the

velocity vector x. Basically, we need to know to which vector in \Box^p it is taken by d(GoF). the curve (GoF)(x(t) = G(F(x(t))). By the same theorem, it equals the image under dG of the Anycast Flow vector to the curve F(x(t)) in \Box^m . Applying the theorem once again, we see that the velocity vector to the curve F(x(t)) is the image under dF of the vector x(t). Hence d(GoF)(x) = dG(dF(x)) for an arbitrary vector x.

Corollary 1.0. If we denote coordinates in \Box^n by $(x^1, ..., x^n)$ and in \Box^m by $(y^1, ..., y^m)$, and write $dF = \frac{\partial F}{\partial x^1} dx^1 + ... + \frac{\partial F}{\partial x^n} dx^n \qquad (1)$

$$dG = \frac{\partial G}{\partial y^1} dy^1 + \dots + \frac{\partial G}{\partial y^n} dy^n, \qquad (2)$$

Then the chain rule can be expressed as follows: $d(GoF) = \frac{\partial G}{\partial y^1} dF^1 + \dots + \frac{\partial G}{\partial y^m} dF^m,$ (3)

Where dF^i are taken from (1). In other words, to get d(GoF) we have to substitute into (2) the expression for $dy^i = dF^i$ from (3). This can also be expressed by the following matrix formula:

$$d(GoF) = \begin{pmatrix} \frac{\partial G^{1}}{\partial y^{1}} \cdots \frac{\partial G^{1}}{\partial y^{m}} \\ \cdots & \cdots & \cdots \\ \frac{\partial G^{p}}{\partial y^{1}} \cdots \frac{\partial G^{p}}{\partial y^{m}} \end{pmatrix} \begin{pmatrix} \frac{\partial F^{1}}{\partial x^{1}} \cdots \frac{\partial F^{1}}{\partial x^{n}} \\ \cdots & \cdots & \cdots \\ \frac{\partial F^{m}}{\partial x^{1}} \cdots \frac{\partial F^{m}}{\partial x^{n}} \end{pmatrix} \begin{pmatrix} dx^{1} \\ \cdots \\ dx^{n} \end{pmatrix}$$
(4)

i.e., if dG and dF are expressed by matrices of partial derivatives, then d(GoF) is expressed by the product of these matrices. This is often written as

$$\begin{pmatrix} \frac{\partial z^{1}}{\partial x^{1}} \cdots \frac{\partial z^{1}}{\partial x^{n}} \\ \cdots & \cdots & \cdots \\ \frac{\partial z^{p}}{\partial x^{1}} \cdots \frac{\partial z^{p}}{\partial x^{n}} \end{pmatrix} = \begin{pmatrix} \frac{\partial z^{1}}{\partial y^{1}} \cdots \frac{\partial z^{1}}{\partial y^{m}} \\ \cdots & \cdots & \cdots \\ \frac{\partial z^{p}}{\partial y^{1}} \cdots \frac{\partial y^{1}}{\partial x^{n}} \\ \cdots & \cdots & \cdots \\ \frac{\partial y^{m}}{\partial x^{1}} \cdots \frac{\partial y^{m}}{\partial x^{n}} \end{pmatrix}, \qquad (5)$$
Or
$$\frac{\partial z^{\mu}}{\partial x^{a}} = \sum_{i=1}^{m} \frac{\partial z^{\mu}}{\partial y^{i}} \frac{\partial y^{i}}{\partial x^{a}}, \qquad (6)$$

Where it is assumed that the dependence of $y \in \square^m$ on $x \in \square^n$ is given by the map F, the dependence of $z \in \square^p$ on $y \in \square^m$ is given by the map G, and the dependence of $z \in \square^p$ on $x \in \square^n$ is given by the composition GoF.

Definition 1.6. Consider an open domain $U \subset \square^n$. Consider also another copy of \square^n , denoted for distinction \square_y^n , with the standard coordinates $(y^1...y^n)$. A system of coordinates in the open domain U is given by a map $F: V \to U$, where $V \subset \square_y^n$ is an open domain of \square_y^n , such that the following three conditions are satisfied :

- (1) F is smooth;
- (2) F is invertible;

(3) $F^{-1}: U \to V$ is also smooth

The coordinates of a point $x \in U$ in this system are the standard coordinates of $F^{-1}(x) \in \prod_{y=1}^{n} \sum_{y=1}^{n} \sum_{y=1$

$$F:(y^{1}...,y^{n})\mapsto x=x(y^{1}...,y^{n})$$
 (1)

Here the variables $(y^1..., y^n)$ are the "new" coordinates of the point x

Example 1.2. Consider a curve in \square^2 specified in polar coordinates as



 $x(t): r = r(t), \varphi = \varphi(t)$ (1)

We can simply use the chain rule. The map $t \mapsto x(t)$ can be considered as the composition of the maps $t \mapsto (r(t), \varphi(t)), (r, \varphi) \mapsto x(r, \varphi)$. Then, by the chain rule, we have

$$x = \frac{dx}{dt} = \frac{\partial x}{\partial r}\frac{dr}{dt} + \frac{\partial x}{\partial \varphi}\frac{d\varphi}{dt} = \frac{\partial x}{\partial r}r + \frac{\partial x}{\partial \varphi}\varphi$$
(2)

Here r and ϕ are scalar coefficients depending on

t, whence the partial derivatives $\frac{\partial x}{\partial r}, \frac{\partial x}{\partial \varphi}$ are

vectors depending on point in \Box^2 . We can compare this with the formula in the "standard" coordinates:

$$x = e_1 x + e_2 y \quad \text{Consider} \quad \text{the vectors}$$

$$\frac{\partial x}{\partial r}, \frac{\partial x}{\partial \varphi}, \text{ Explicitly we have}$$

$$\frac{\partial x}{\partial r} = (\cos \varphi, \sin \varphi) \quad (3)$$

$$\frac{\partial x}{\partial \varphi} = (-r \sin \varphi, r \cos \varphi) \quad (4)$$

From where it follows that these vectors make a basis at all points except for the origin (where r = 0). It is instructive to sketch a picture, drawing vectors corresponding to a point as starting from that point. Notice that $\frac{\partial x}{\partial r}, \frac{\partial x}{\partial \varphi}$ are, respectively, the velocity vectors for the curves $r \mapsto x(r, \varphi)$ ($\varphi = \varphi_0 \ fixed$) and $\varphi \mapsto x(r, \varphi) \ (r = r_0 \ fixed)$. We can conclude

that for an arbitrary curve given in polar coordinates

the velocity vector will have components (r, φ) if

as a basis we take $e_r := \frac{\partial x}{\partial r}, e_{\varphi} := \frac{\partial x}{\partial \varphi}$:

$$\dot{x} = e_r r + e_\varphi \varphi \tag{5}$$

A characteristic feature of the basis e_r, e_{φ} is that it is not "constant" but depends on point. Vectors "stuck to points" when we consider curvilinear coordinates.

Proposition 1.3. The velocity vector has the same appearance in all coordinate systems.

Proof. Follows directly from the chain rule and the transformation law for the basis e_i . In particular, the elements of the basis $e_i = \frac{\partial x}{\partial x^i}$ (originally, a formal notation) can be understood directly as the velocity vectors of the coordinate lines

 $x^i \mapsto x(x^1, ..., x^n)$ (all coordinates but x^i are fixed). Since we now know how to handle velocities in arbitrary coordinates, the best way to treat the differential of a map $F : \square^n \to \square^m$ is by its action on the velocity vectors. By definition, we set

$$dF(x_0):\frac{dx(t)}{dt}(t_0)\mapsto \frac{dF(x(t))}{dt}(t_0) \tag{1}$$

Now $dF(x_0)$ is a linear map that takes vectors attached to a point $x_0 \in \square^n$ to vectors attached to the point $F(x) \in \square^m$

$$dF = \frac{\partial F}{\partial x^{1}} dx^{1} + \dots + \frac{\partial F}{\partial x^{n}} dx^{n}$$

$$(e_{1}, \dots, e_{m}) \begin{pmatrix} \frac{\partial F^{1}}{\partial x^{1}} \dots \frac{\partial F^{1}}{\partial x^{n}} \\ \dots & \dots & \dots \\ \frac{\partial F^{m}}{\partial x^{1}} \dots \frac{\partial F^{m}}{\partial x^{n}} \end{pmatrix} \begin{pmatrix} dx^{1} \\ \dots \\ dx^{n} \end{pmatrix}, \qquad (2)$$

In particular, for the differential of a function we always have

$$df = \frac{\partial f}{\partial x^1} dx^1 + \dots + \frac{\partial f}{\partial x^n} dx^n, \qquad (3)$$

Where x^{i} are arbitrary coordinates. The form of the differential does not change when we perform a change of coordinates.

Example 1.3 Consider a 1-form in \square^2 given in the standard coordinates:

A = -ydx + xdy In the polar coordinates we will have $x = r \cos \varphi$, $y = r \sin \varphi$, hence $dx = \cos \varphi dr - r \sin \varphi d\varphi$ $dy = \sin \varphi dr + r \cos \varphi d\varphi$ Substituting into A, we get $A = -r \sin \varphi (\cos \varphi dr - r \sin \varphi d\varphi)$ $+r \cos \varphi (\sin \varphi dr + r \cos \varphi d\varphi)$ $= r^2 (\sin^2 \varphi + \cos^2 \varphi) d\varphi = r^2 d\varphi$ Hence $A = r^2 d\varphi$ is the formula for A in the polar coordinates. In particular, we see that this is again a 1-form, a linear combination of the differentials of coordinates with functions as

differentials of coordinates with functions as coefficients. Secondly, in a more conceptual way, we can define a 1-form in a domain U as a linear function on vectors at every point of U: $\omega(v) = \omega_1 v^1 + ... + \omega_n v^n$, (1)



If $\upsilon = \sum e_i \upsilon^i$, where $e_i = \frac{\partial x}{\partial x^i}$. Recall that the differentials of functions were defined as linear functions on vectors (at every point), and $dx^i(e_j) = dx^i \left(\frac{\partial x}{\partial x^j}\right) = \delta_j^i$ (2) at

every point x.

Theorem 1.9. For arbitrary 1-form ω and path γ , the integral $\int_{\gamma} \omega$ does not change if we change parametrization of γ provide the orientation remains the same.

Proof: Consider
$$\left\langle \omega(x(t)), \frac{dx}{dt} \right\rangle$$
 and $\left\langle \omega(x(t(t'))), \frac{dx}{dt} \right\rangle$ As $\left\langle \omega(x(t(t'))), \frac{dx}{dt} \right\rangle = \left| \left\langle \omega(x(t(t'))), \frac{dx}{dt} \right\rangle \cdot \frac{dt}{dt} \right\rangle$

Let p be a rational prime and let $K = \Box (\zeta_p)$. We write ζ for ζ_p or this section. Recall that K has degree $\varphi(p) = p - 1$ over \Box . We wish to show that $O_K = \Box [\zeta]$. Note that ζ is a root of $x^p - 1$, and thus is an algebraic integer; since O_K is a ring we have that $\Box [\zeta] \subseteq O_K$. We give a proof without assuming unique factorization of ideals. We begin with some norm and trace computations. Let j be an integer. If j is not divisible by p, then ζ^j is a primitive p^{th} root of unity, and thus its conjugates are $\zeta, \zeta^2, ..., \zeta^{p-1}$. Therefore

 $Tr_{K/\Box}(\zeta^{j}) = \zeta + \zeta^{2} + ... + \zeta^{p-1} = \Phi_{p}(\zeta) - 1 = -1$ If *p* does divide *j*, then $\zeta^{j} = 1$, so it has only the one conjugate 1, and $Tr_{K/\Box}(\zeta^{j}) = p - 1$ By linearity of the trace, we find that

$$Tr_{K/\Box} (1 - \zeta) = Tr_{K/\Box} (1 - \zeta^2) = \dots$$

= $Tr_{K/\Box} (1 - \zeta^{p-1}) = p$

We also need to compute the norm of $1-\zeta$. For this, we use the factorization

$$x^{p-1} + x^{p-2} + \dots + 1 = \Phi_p(x)$$

= $(x - \zeta)(x - \zeta^2) \dots (x - \zeta^{p-1});$

Plugging in x = 1 shows that

 $p = (1 - \zeta)(1 - \zeta^2) \dots (1 - \zeta^{p-1})$

Since the $(1-\zeta^{j})$ are the conjugates of $(1-\zeta)$, this shows that $N_{K/\Box}(1-\zeta) = p$ The key result for determining the ring of integers O_{K} is the following.

LEMMA 1.9

 $(1 - \zeta)O_{\kappa} \cap \Box = p\Box$

Proof. We saw above that p is a multiple of $(1-\zeta)$ in O_K , so the inclusion $(1-\zeta)O_K \cap \Box \supseteq p\Box$ is immediate. Suppose now that the inclusion is strict. Since $(1-\zeta)O_K \cap \Box$ is an ideal of \Box containing $p\Box$ and $p\Box$ is a maximal ideal of \Box , we must have $(1-\zeta)O_K \cap \Box = \Box$ Thus we can write $1 = \alpha(1-\zeta)$

For some $\alpha \in O_K$. That is, $1-\zeta$ is a unit in O_K .

COROLLARY 1.1 For any $\alpha \in O_K$, $Tr_{K/\Box} ((1-\zeta)\alpha) \in p\Box$ PROOF. We have

$$Tr_{K/\Box} ((1-\zeta)\alpha) = \sigma_1((1-\zeta)\alpha) + \dots + \sigma_{p-1}((1-\zeta)\alpha)$$

= $\sigma_1(1-\zeta)\sigma_1(\alpha) + \dots + \sigma_{p-1}(1-\zeta)\sigma_{p-1}(\alpha)$
= $(1-\zeta)\sigma_1(\alpha) + \dots + (1-\zeta^{p-1})\sigma_{p-1}(\alpha)$

Where the σ_i are the complex embeddings

of K (which we are really viewing as automorphisms of K) with the usual ordering. Furthermore, $1-\zeta^{j}$ is a multiple of $1-\zeta$ in O_{K} for every $j \neq 0$. Thus $Tr_{K/\Box} (\alpha(1-\zeta)) \in (1-\zeta)O_{K}$ Since the trace is

 $Ir_{K/\Box}(\alpha(1-\zeta)) \in (1-\zeta)O_K$ Since the trace is also a rational integer.

PROPOSITION 1.4 Let p be a prime number and let $K = |\Box (\zeta_p)$ be the p^{th} cyclotomic field. Then $O_K = \Box [\zeta_p] \cong \Box [x] / (\Phi_p(x));$ Thus $1, \zeta_p, ..., \zeta_p^{p-2}$ is an integral basis for O_K . PROOF. Let $\alpha \in O_K$ and write $\alpha = a_0 + a_1 \zeta + ... + a_{p-2} \zeta^{p-2}$ With $a_i \in \Box$. Then



$$\alpha(1-\zeta) = a_0(1-\zeta) + a_1(\zeta-\zeta^2) + \dots + a_{p-2}(\zeta^{p-2}-\zeta^{p-1})$$

By the linearity of the trace and our above calculations we find that $Tr_{K/\Box}(\alpha(1-\zeta)) = pa_0$ We also have

 $Tr_{K/\Box} (\alpha(1-\zeta)) \in p\Box$, so $a_0 \in \Box$ Next consider the algebraic integer

 $(\alpha - a_0)\zeta^{-1} = a_1 + a_2\zeta + ... + a_{p-2}\zeta^{p-3}$; This is an algebraic integer since $\zeta^{-1} = \zeta^{p-1}$ is. The same argument as above shows that $a_1 \in \Box$, and continuing in this way we find that all of the a_i are in \Box . This completes the proof.

Example 1.4 Let $K = \Box$, then the local ring $\Box_{(p)}$ is simply the subring of \Box of rational numbers with denominator relatively prime to p. Note that this ring $\Box_{(p)}$ is not the ring \Box_p of padic integers; to get \square_p one must complete $\square_{(p)}$. The usefulness of $O_{K,p}$ comes from the fact that it has a particularly simple ideal structure. Let a be any proper ideal of $O_{K,p}$ and consider the ideal $a \cap O_{\kappa}$ of O_{κ} . We claim that $a = (a \cap O_K)O_{K,n}$; That is, that a is generated by the elements of a in $a \cap O_{K}$. It is clear from the definition of an ideal that $a \supseteq (a \cap O_{\kappa})O_{\kappa_n}$. To prove the other inclusion, let α be any element of *a*. Then we can write $\alpha = \beta / \gamma$ where $\beta \in O_{\kappa}$ and $\gamma \notin p$. In particular, $\beta \in a$ (since $\beta / \gamma \in a$ and a is an ideal), so $\beta \in O_K$ and $\gamma \notin p$. so $\beta \in a \cap O_K$. Since $1/\gamma \in O_{K,p}$, this implies that $\alpha = \beta / \gamma \in (\alpha \cap O_K)O_{K_n}$, as claimed.We can use this fact to determine all of the ideals of $O_{K,p}$. Let *a* be any ideal of $O_{K,p}$ and consider the ideal factorization of $a \cap O_{\kappa}$ in O_{κ} . write it as $a \cap O_{K} = p^{n}b$ For some *n* and some ideal b, relatively prime to p, we claim first that $bO_{K,p} = O_{K,p}$. We now find that

$$a = (a \cap O_K)O_{K,p} = p^n bO_{K,p} = p^n O_{K,p}$$

Since $bO_{K,p}$. Thus every ideal of $O_{K,p}$ has the form $p^nO_{K,p}$ for some *n*; it follows immediately

that $O_{K,p}$ is noetherian. It is also now clear that $p^n O_{K,p}$ is the unique non-zero prime ideal in $O_{K,p}$. Furthermore, the inclusion $O_K \mapsto O_{K,p} / pO_{K,p}$ Since $pO_{K,p} \cap O_K = p$, this map is also surjection, since the residue class of $\alpha / \beta \in O_{\kappa_n}$ (with $\alpha \in O_K$ and $\beta \notin p$) is the image of $\alpha \beta^{-1}$ in $O_{K/p}$, which makes sense since β is invertible in $O_{K/p}$. Thus the map is an isomorphism. In particular, it is now abundantly clear that every nonzero prime ideal of $O_{K,p}$ is maximal. То show that $O_{K,p}$ is a Dedekind domain, it remains to show that it is integrally closed in K. So let $\gamma \in K$ be a root of a polynomial with coefficients in write this polynomial $O_{K_n};$ as $x^m + \frac{\alpha_{m-1}}{\beta_{m-1}} x^{m-1} + \ldots + \frac{\alpha_0}{\beta_0}$ With $\alpha_i \in O_K$ and $\beta_i \in O_{K-n}$. Set $\beta = \beta_0 \beta_1 \dots \beta_{m-1}$. Multiplying by β^m we find that $\beta\gamma$ is the root of a monic polynomial with coefficients in O_{κ} . Thus $\beta \gamma \in O_{\kappa};$ since $\beta \notin p$, we have $\beta \gamma / \beta = \gamma \in O_{K,p}$. Thus $O_{K,p}$ is integrally close in K.

COROLLARY 1.2. Let *K* be a number field of degree *n* and let α be in O_K then $N'_{K/\Box}(\alpha O_K) = |N_{K/\Box}(\alpha)|$

PROOF. We assume a bit more Galois theory than usual for this proof. Assume first that K/\Box is Galois. Let σ be an element of $Gal(K/\Box)$. It is $\sigma(O_{K}) / \sigma(\alpha) \cong O_{K/\alpha};$ clear that since $\sigma(O_{\kappa}) = O_{\kappa},$ this shows that $\dot{N_{K/\square}}(\sigma(lpha)O_{K}) = N_{K/\square}(lpha O_{K})$. Taking the product over all $\sigma \in Gal(K/\Box)$, we have $N_{K/\Gamma}(N_{K/\Gamma}(\alpha)O_{K}) = N_{K/\Gamma}(\alpha O_{K})^{n}$ Since $N_{_{K/\square}}(\alpha)$ is a rational integer and $O_{_K}$ is a free \square module of rank n,

 $O_{_K} / N_{_{K/\!\square}}(\alpha) O_{_K}$ Will have order $N_{_{K/\!\square}}(\alpha)^n$; therefore

$$N_{K/\Box}^{\prime}(N_{K/\Box}(\alpha)O_{K}) = N_{K/\Box}(\alpha O_{K})^{\prime}$$



This completes the proof. In the general case, let L be the Galois closure of K and set [L:K] = m.

G. Application of Smart Grid

The applications in the Smart Grid are divided into smart power generation, intelligent transmission and substation and intelligent power use. Data collection is the key to intelligentize power grid. Realization of intelligent power grid makes it possible to get the information of the intelligent power grid completely and in time. The control of the grid information needs perfect communication lines and enough terminal information, and it can ensure the security and stability of data transmission, improve the reliability of data exchange and provide accurate information in time for the intelligent application. Smart Grid may use more devices, including a variety of intelligent sensors, control components and electrical equipment, which require higher digitization degree of power grid and better data collection, transmission, storage and utilization in the process of power generation, transmission, substation and distribution. Using a variety of information collection technologies to collect information of power use and device status and get the equipment running status make it possible to get the information of equipment failure in time, which can ensure the equipment operate correctly[17]. Some of the information collection technologies are based on Power Line Carrier Communication, some are based on fiber network, some are based on cable transmission, and others are based on wireless transmission. Because networks and users are various, especially in power using side, there are no network transmission ways that can meet the demands of all kinds of users. Suitable methods should be selected according to different demands. For wireless communication can be installed fast and need no line, it can be used in areas where network infrastructure are not so developed or can not be developed, such as old town, mountain areas and vast rural areas. Therefore, the research work on wireless sensor network applications in the smart grid is useful complement to cable transmission. For the features of the low-cost and low power consumption in user managing and Meter Reading, Zigbee is often used in Automatic Meter Reading. But Zigbee has limitations too, such as low capacity of NLOS transmission, which is fatal to meter data collection in thousands of families of high-rise apartment-style. And more, its transmission rate is too low to meet the demands of the new generation of Automatic Meter Reading system in large scale of data realtime transmission and control. Comparing with Zigbee-based WSN, WiFi-based WSN has better NLOS transmission capability and can be used to transmit through the load-bearing walls. It is more suitable for thousands of families meter reading transmission in high-rise apartment-style. More, its transmission rate is faster and its bandwidth is higher, so it is more suitable for the new generation Internet of Things-based Automatic Meter Reading system, which has large scale of real-time data. In addition, WiFi is securer and WiFi-based WSN has lower power consumption comparing with Zigbee. Therefore, WiFi sensor network is more suitable to build new generation Automatic Meter Reading system facing to Internet of Things. With the increasing of production, the product cost of WiFibase WSN will decrease soon. With the continuous development of SOC technology, the power consumption of WiFi sensor chip will be further reduced and it will be more suitable for Automatic Meter Reading or other applications which need low power consumption.

IV. WSN BASED HOME ENERGY MANAGEMENT APPLICATIONS

In the smart grid, HANs will become the natural extensions of the grid penetrating into the residential areas, and home energy management will be a part of the coordination between generation and load. In [12], we presented an in-Home Energy Management (iHEM) application that uses WSNs. In this paper, we present detailed performance evaluation of the WSN used in iHEM. The iHEM smart appliances application employs with communication capability, a WSN and a central Energy Management Unit (EMU). In the iHEM application, when a consumer turns on an appliance, the appliance generates a START-REQ packet and sends it to the EMU. When the EMU receives the START-REQ packet, it sends AVAIL-REQ packets to the energy storage units to retrieve the amount of energy generated by the renewable resources and stored in their associated storage units. EMU also communicates with the smart meter periodically and receives updated price information from the utility. Upon reception of AVAIL-REQ, the storage unit replies with a AVAIL-REP packet where the amount of available energy is sent to the EMU. After receiving the AVAILREP packet, EMU determines the convenient starting time of the appliance. Basically EMU first tries to accommodate the appliance requests by the locally generated power. If the local power is not adequate then it tries to shift the request to an off-peak hour. After these scheduling attempts, EMU computes the waiting time as the difference between the suggested and requested start time, and sends the waiting time in the START-REP packet to the appliance. The waiting time is displayed on the LCD monitor of the appliance. The consumer decides whether to start the appliance right away or wait until the assigned time slot depending on the waiting time. The decision of the consumer is sent back to the EMU with a NOTIFICATION packet. This handshake protocol among the appliance and the EMU ensures that EMU does not force an automated start time which avoids degrading the comfort of the consumers and provides



flexibility. The iHEM application utilizes a WSN to relay its packets. We assume that this WSN is also utilized for other applications in the smart home. The WSN continues its regular tasks, such as inhabitant health monitoring, and at the same time, it relays iHEM messages. The WSN communicates via Zigbee. A sample topology of the WSN is given in Figure 3. Zigbee is a short-range, low-data rate, energy-efficient wireless technology that is based on the IEEE 802.15.4 standard. Zigbee utilizes 16 channels in the 2.4GHz ISM band worldwide, 13 channels in the 915MHz band in North America and one channel in the 868MHz band in Europe. The supported data rates are 250 kbps, 40 kbps, and 20 kbps. Zigbee's range is approximately 30 meters indoors. It supports 16-bit and 64- bit addressing modes, and it can support up to 64,000 nodes (devices). However, when HAN devices need to get integrated with the Internet, IP addressing is required. IPv6 over Low- Power Wireless Personal Area Networks (6LoWPAN), which is defined in the IETF RFC 4944, aims to integrate IPv6 addressing to LoWPANs like Zigbee. 6LoWPAN adds an adaptation layer to handle fragmentation, reassembly and header compression issues, to support IPv6 packets on the short packet structure of Zigbee. Zigbee allows two types of devices which are Full Function Device (FFD) and Reduced Function Device (RFD). FFDs can communicate with their peers while RFDs are simpler than FFDs and they can be the edge nodes in a star topology. In Zigbee, sensor nodes are either organized in a star topology, mesh topology or a cluster-tree topology. In our model home, the WSN is organized in a cluster-tree topology. Zigbee requires a Personal Area Network (PAN) coordinator. PAN coordinator can operate in beacon-enabled mode or beaconless mode. The duty cycle of the nodes is defined with the superframe duration (SD) of the superframe structure. A superframe synchronizes the nodes in the network and nodes. Superframe has Contention Access Period (CAP) and Contention Free Period (CFP) slots. During CAP, nodes compete to access the channel by using the slotted Carrier Sense Multiple Access with Collision Avoidance (CSMA/CA) technique. During CFP, nodes that have previously reserved Guaranteed Time Slots (GTS) transmit their data. One cycle of active and inactive periods can occur within a Beacon Interval (BI) which starts at the beginning of a beacon frame and ends at the beginning of the next beacon frame. SD and BI are calculated as follows [13]

A. Noise and Interference Measurements

In this section, we first investigate the impact of background noise on the overall performance of 802.15.4 sensor networks in different electric-power-system environments. Then, we show the effect of electronic appliances on 802.15.4 sensor networks. To measure background noise, we wrote a

TinyOS application that samples RF energy at 62.5 Hz by reading the received signal strength indicator (RSSI) register of the CC2420 radio. The register contains the average RSSI over the past eight symbol periods. We sampled noise on different radio channels in a wide range of environments, including an indoor power control room, a 500-kV substation, and an underground network transformer vault. Fig. 2 shows our noise measurements and the effect of an electric appliance (microwave oven) on an 802.15.4 network. From the field measurements, the average noise level is found to be around -90 dBm, which is significantly higher than that of outdoor environments, i.e., -105-dBm background noise is found in outdoor environments. We also observe that background noise continuously changes over time, which can be caused by temperature changes and interference levels. In Fig. 2(d), we also show the effect of microwave-oven interference on the noise floor measured by the Tmote Sky module [20]. As shown in Fig. 2, the interference from an existing microwave oven leads to a 15-dBm interference in the 2.4-GHz frequency band.

B. Link-Quality Measurements

In this section, we focused on how to characterize and measure link quality in sensor networks deployed in electric-powersystem environments. We have conducted experiments with Tmote Sky nodes. In our experiments, to measure the radio link quality, two useful radio-hardware linkquality metrics were used: LQI and RSSI. Specifically, RSSI is the estimate of the signal power and is calculated over eight symbol periods, while LQI can be viewed as chip error rate and is calculated over eight symbols following the start frame delimiter. LQI values are usually between 110 and 50 and correspond to maximum and minimum quality frames, respectively. The details of LQI metric can be found in the IEEE 802.15.4 standard [15]. In our experiments, we use a pair of Tmote Sky nodes in different utility environments and outdoor environment, one as the sender and the other as the receiver. We vary the distance from the receiver to the sender from 1 to 20 m, in steps of 1 m. The output power level of each sensor node and the packet size were set to be -25 dBm and 30 B, respectively. At each distance, the transmitter sends 200 data packets with a rate of 2 packets/s. We deliberately chose a low rate to avoid any potential interference, so that the effect of unreliable links can be isolated from that of congestion. In addition, various NLOS communication links are also considered. In Fig. 3, we present our preliminary experiment results to elaborate the relationship between PRR and link-quality metrics. Here, PRR represents the ratio of the number of successful packets to the total number of packets transmitted over a certain number of transmissions. Specifically, Fig. 3 shows 95% confidence intervals. In this figure,



we observe a strong correlation between the average LQI values and PRRs at the receiver. Statistical analysis shows that the Pearson correlation coefficient is around 0.70 between these two variables for the indoor main power room. This correlation implies that average LQI is a good measurable indicator of the packet reception probability. This observation is also consistent with the results in the related literature [20]. In Fig. 3, we also observe that there is a much smaller correlation between RSSI and the packet reception probability. The Pearson correlation coefficient is only 0.50 between the packet reception probability and the RSSI value. Furthermore, it is found that when the signal is weak [particularly when it is around the sensitivity threshold of CC2420(-94 dBm)], even though there is a considerable variation in the packet loss rate, RSSI does not provide any correlated behavior with PRR. Here, it is also important to note that all these measurements should be used as a reference. The exact values for a particular site are likely to vary depending on the actual environment propagation characteristics, RF interference, etc.

C. Applications

With the distributed networked monitoring system, the physical conditions of an overhead transmission line can be quantitatively determined in a real-time manner. The application matrix may include the measurement tension/strain, vibration, tilt, and temperature. With these quantities, some associated phenomena can be predicted, e.g., overheating, vibration, galloping, ice accretion, and sag[18]. These quantities can be used to assess the security of the power transmission system, hence allowing operators to regulate the power transfer on the transmission line, and the authors in [5] even proposed to use the sag measurement to correct the resistance and reactance data for transmission lines. In the past, the sag of the overhead transmission line is evaluated by measuring the strain/tension by placing load cells at the attachment point of conductor. With these information, the sag is evaluated with either catenary equation or its reduced version, i.e., parabolic equation. However, using of catenary equation or parabolic equation has to rely on the hypothesis that the load between a span is uniform. This hypothesis is not always true. A quanlitive observation on the above test setup shows that the detected strain varies largely when applying same amount of strenth at the different location of a span. Fig. 3 and Fig. 4 show the comparison of the strain distribution and sag distribution under uniform load and concentrated load. This figure presents the simulation results by using Ansys®. An conductor (LGJ-400/35) is applied with a concentrated load (at the point x=300), and with same amount of load but distributed uniformed along the transmission line. The parameters of LGJ400-35 conductor are shown in Table II. With the increased observability due to

the distributed measurement, it is possible to predict the sag more accurately. Fig. 4 demonstrate an algorithm to estimate the sag with the distributed measured information. In this model, every section between two measurement points is approximately regarded as a transmission line governed by a catenary equation or reduced parabolic equation. Since the power transmission line is flexible with certain high rigidity, such dealment is resonable. The sags of the whole transmission line are evaluated with a series of catenary equations or reduced parabolic equations. Evaluation shows that a point on the transmission line does not move much along horizontal direction (i.e., x axis) even with the presence of sag. This is understandable because the stretching of the conductors is limited. Hence, the position of the sensors installed on transmission line can be assumed to be fixed with respect to the x axis.

D. Managing Smart Homes Renewable Energy

Integration of renewable resources are considered as one of the most important goals of the smart grid. Energy generated by means of solar power, wind power, etc., can be stored for future use by the home appliances or it can be sold to the grid. Our application manages the usage and flow of the energy, and keeps track of the smart home energy usage performance. In this application, we consider three cases: i) the home is using electricity from the grid even it might have energy on the storage devices, ii) the home quits using electricity from the grid and uses locally generated or stored energy, iii) the home sells electricity to the grid. In our application, the user may choose to do one of the above actions depending on the price of electricity and the amount of energy stored. The utility applies rates that vary with the time of day which is called as Time Of Use(TOU) billing. In our application, the best time to switch between any of the above three scenarios is chosen automatically. For the above scenarios, we assume the system has a storage device combined with the sensor node to get the current saved energy amount. The sensor node carry the flow management system to coordinate when to use the stored energy, furthermore it decides wether to sell electricity back to the grid or not, depending on the amount of energy already exists on the storage device. This system is fully automated, since the inhabitant might be out of the home and there is electricity in the storage device, so in this case the system could work independently and benefit from the energy without waiting for the user interaction. However the inhabitant might configure the system and change its default configuration by assigning the peak hours and amount of energy the house needs every day.

In the default case, energy is supplied from the grid. When the renewable energy is stored in adequate amounts then energy can be supplied from the storage device. On the other hand, when there is excess energy store, the user can sell electricity to the utility. The selection of the energy supply and the decision whether to consume or to sell the energy to the grid can be controlled by the application illustrate in Algorithm 2. The algorithm starts by asking the current time, if it does not belong to the peak hours already configured by the home owner, then the algorithm terminates, and the home keeps using the grid energy. Otherwise, the algorithm gets the amount of energy from the storage that exceeds the home needs for one day. If that amount is greater than zero, it is sold back to the grid and the home start using it needs from the storage device. Otherwise the home does not sell any amount back. and stop using the grid power, and the storage start supplying the home with the stored energy. The described system works in the storage device sensor node in the smart home to manage the usage of the electricity flow. Furthermore, the utility integrates this application to its customer management system, in order to take the amount of the renewable energy the house benefit. This information can be used to provide better rates for the customer who employs more renewable energy.

E. Authors and Affiliations

Dr Akash Singh is working with IBM Corporation as an IT Architect and has been designing Mission Critical System and Service Solutions; He has published papers in IEEE and other International Conferences and Journals.

He joined IBM in Jul 2003 as a IT Architect which conducts research and design of High Performance Smart Grid Services and Systems and design mission critical architecture for High Performance Computing Platform and Computational Intelligence and High Speed Communication systems. He is a member of IEEE (Institute for Electrical and Electronics Engineers), the AAAI (Association for the Advancement of Artificial Intelligence) and the AACR (American Association for Cancer Research). He is the recipient of numerous awards from World Congress in Computer Science, Computer Engineering and Applied Computing 2010, 2011, and IP Multimedia System 2008 and Billing and Roaming 2008. He is active research in the field of Artificial Intelligence and advancement in Medical Systems. He is in Industry for 18 Years where he performed various role to provide the Leadership in Information Technology and Cutting edge Technology.

REFERENCES

- Dynamics and Control of Large Electric Power Systems. Ilic, M. and Zaborszky, J. John Wiley & Sons, Inc. © 2000, p. 756.
- [2] Modeling and Evaluation of Intrusion Tolerant Systems Based on Dynamic Diversity Backups. Meng, K. et al. Proceedings of the 2009 International

Symposium on Information Processing (ISIP'09). Huangshan, P. R. China, August 21-23, 2009, pp. 101–104

- [3] Characterizing Intrusion Tolerant Systems Using A State Transition Model. Gong, F. et al., April 24, 2010.
- [4] Energy Assurance Daily, September 27, 2007. U.S. Department of Energy, Office of Electricity Delivery and Energy Reliability, Infrastructure Security and Energy Restoration Division. April 25, 2010.
- [5] CENTIBOTS Large Scale Robot Teams. Konoledge, Kurt et al. Artificial Intelligence Center, SRI International, Menlo Park, CA 2003.
- [6] Handling Communication Restrictions and Team Formation in Congestion Games, Agogino, A. and Tumer, K. Journal of Autonomous Agents and Multi Agent Systems, 13(1):97–115, 2006.
- [7] Robotics and Autonomous Systems Research, School of Mechanical, Industrial and Manufacturing Engineering, College of Engineering, Oregon State University
- [8] D. Dietrich, D. Bruckner, G. Zucker, and P. Palensky, "Communication and computation in buildings: A short introduction and overview," *IEEE Trans. Ind. Electron.*, vol. 57, no. 11, pp. 3577– 3584, Nov. 2010.
- [9] V. C. Gungor and F. C. Lambert, "A survey on communication networks for electric system automation," *Comput. Networks*, vol. 50, pp. 877–897, May 2006.
- [10] S. Paudyal, C. Canizares, and K. Bhattacharya, "Optimal operation of distribution feeders in smart grids," *IEEE Trans. Ind. Electron.*, vol. 58, no. 10, pp. 4495–4503, Oct. 2011.
- [11] D. M. Laverty, D. J. Morrow, R. Best, and P. A. Crossley, "Telecommunications for smart grid: Backhaul solutions for the distribution network," in *Proc. IEEE Power* and Energy Society General Meeting, Jul. 25–29, 2010, pp. 1–6.
- [12] L. Wenpeng, D. Sharp, and S. Lancashire, "Smart grid communication network capacity planning for power utilities," in *Proc. IEEE PES, Transmission Distrib. Conf. Expo.*, Apr. 19–22, 2010, pp. 1–4.
- [13] Y. Peizhong, A. Iwayemi, and C. Zhou, "Developing ZigBee deployment guideline under WiFi interference for smart grid applications," *IEEE Trans. Smart Grid*, vol. 2, no. 1, pp. 110–120, Mar. 2011.
- [14] C. Gezer and C. Buratti, "A ZigBee smart energy implementation for energy efficient buildings," in *Proc. IEEE 73rd Veh. Technol. Conf. (VTC Spring)*, May 15–18, 2011, pp. 1–5.



- [15] R. P. Lewis, P. Igic, and Z. Zhongfu, "Assessment of communication methods for smart electricity metering in the U.K.," in *Proc. IEEE PES/IAS Conf. Sustainable Alternative Energy (SAE)*, Sep. 2009, pp. 1–4.
- [16] A. Yarali, "Wireless mesh networking technology for commercial and industrial customers," in *Proc. Elect. Comput. Eng.*, *CCECE*,May 1–4, 2008, pp. 000047– 000052.
- [17] M. Y. Zhai, "Transmission characteristics of low-voltage distribution networks in China under the smart grids environment," *IEEE Trans. Power Delivery*, vol. 26, no. 1, pp. 173–180, Jan. 2011.
- [18] V. Paruchuri, A. Durresi, and M. Ramesh, "Securing powerline communications," in *Proc. IEEE Int. Symp. Power Line Commun. Appl.*, (ISPLC), Apr. 2–4, 2008, pp. 64–69.
- [19] Q.Yang, J. A. Barria, and T. C. Green, "Communication infrastructures for distributed control of power distribution networks," *IEEE Trans. Ind. Inform.*, vol. 7, no. 2, pp. 316–327, May 2011.
- [20] T. Sauter and M. Lobashov, "End-to-end communication architecture for smart grids," *IEEE Trans. Ind. Electron.*, vol. 58, no. 4, pp. 1218–1228, Apr. 2011.
- [21] K. Moslehi and R. Kumar, "Smart grid—A reliability perspective," *Innovative Smart Grid Technologies (ISGT)*, pp. 1–8, Jan. 19–21, 2010.
- [22] Southern Company Services, Inc., "Comments request for information on smart grid communications requirements," Jul. 2010
- [23] R. Bo and F. Li, "Probabilistic LMP forecasting considering load uncertainty," *IEEE Trans. Power Syst.*, vol. 24, pp. 1279–1289, Aug. 2009.

- [24] Power Line Communications, H. Ferreira, L. Lampe, J. Newbury, and T. Swart (Editors), Eds. New York: Wiley, 2010.
- [25] G. Bumiller, "Single frequency network technology for fast ad hoc communication networks over power lines," WiKu-Wissenschaftsverlag Dr. Stein 2010.
- [31] G. Bumiller, L. Lampe, and H. Hrasnica, "Power line communications for large-scale control and automation systems," *IEEE Commun. Mag.*, vol. 48, no. 4, pp. 106– 113, Apr. 2010.
- [32] M. Biagi and L. Lampe, "Location assisted routing techniques for power line communication in smart grids," in *Proc. IEEE Int. Conf. Smart Grid Commun.*, 2010, pp. 274–278.
- [33] J. Sanchez, P. Ruiz, and R. Marin-Perez, "Beacon-less geographic routing made partical: Challenges, design guidelines and protocols," *IEEE Commun. Mag.*, vol. 47, no. 8, pp. 85–91, Aug. 2009.
- [34] N. Bressan, L. Bazzaco, N. Bui, P. Casari, L. Vangelista, and M. Zorzi, "The deployment of a smart monitoring system using wireless sensors and actuators networks," in *Proc. IEEE Int. Conf. Smart Grid Commun. (SmartGridComm)*, 2010, pp. 49–54.
- [35] S. Dawson-Haggerty, A. Tavakoli, and D. Culler, "Hydro: A hybrid routing protocol for low-power and lossy networks," in *Proc. IEEE Int. Conf. Smart Grid Commun.* (*SmartGridComm*), 2010, pp. 268–273.
- [36] S. Goldfisher and S. J. Tanabe, "IEEE 1901 access system: An overview of its uniqueness and motivation," *IEEE Commun. Mag.*, vol. 48, no. 10, pp. 150– 157, Oct. 2010.
- [37] V. C. Gungor, D. Sahin, T. Kocak, and S. Ergüt, "Smart grid communications and networking," Türk Telekom, Tech. Rep. 11316-01, Apr 2011.